

The Performance of Homeostatic Controller Motifs Dealing with Perturbations of Rapid Growth and Depletion

Supporting Information SI1-SI9

Gunhild Fjeld,¹ Kristian Thorsen,² Tormod Drengstig,²
and Peter Ruoff¹

¹Centre for Organelle Research

²Department of Electrical Engineering and Computer Science,
University of Stavanger, Stavanger, Norway

Supporting Information 1

Responsiveness of Autocatalytic Controllers

A problem the autocatalytic implementation of integral control sometimes faces is that low concentrations of the controller variables E_o or E_i may lead to unresponsive or slow responding controllers. The situation is illustrated in Fig. S1 using combined controller motifs 1 and 5 with the three different kinetic implementations of integral control. In the left panel of Fig. S1a integral control is based on zero-order kinetics with respect to E_i/E_o , while in the middle and right panels integral control is based on first-order and second-order autocatalysis, respectively. Rate constants have been chosen in such a way that the inflow controllers have set-points at $A_{set}^{E_i}=3.0$, while the outflow controllers have set-points at $A_{set}^{E_o}=6.0$. In this arrangement controllers 1 and 5 act as antagonistic pairs as often found in biology (1, 2). Dependent whether inflow perturbations k_1 or outflow perturbations k_2 dominate A is either kept at $A_{set}^{E_o}=6.0$ or $A_{set}^{E_i}=3.0$, respectively.

During the first phase (Figs. S1b and S1c) all three combined controllers are at their steady states with a dominating outflow perturbation in A ($k_1=0.0$, $k_2=1.0$), where A levels are kept at $A_{set}^{E_i}=3.0$. These steady states are maintained by the E_i 's, which for each of the combined controller pairs provide the necessary compensating flux $j_6=k_6 \cdot E_i$ to keep A at $A_{set}^{E_i}=3.0$. In Fig. S1b the concentrations of all E_o 's during the first phase are zero ($k_{11}=k_{12}=k_{13}=k_{14}=0.0$) and make no contributions to the concentrations of A , while in Fig. S1c the autocatalytic controllers are kept during the first phase at a resting level because of $k_{11}=k_{12}=k_{13}=k_{14}=0.01$.

At time $t=5.0$ (start of the second phase) the perturbation profile changes from a dominating outflow perturbation in A to a large constant inflow perturbation ($k_1=10.0$, $k_2=0.0$). While the controller based on zero-order kinetics can compensate for the perturbation by increasing its E_o , the autocatalytic controller species E_o cannot build up (bottom panel, Fig. S1b) with the result that the A levels for these controllers rise rapidly above $A_{set}^{E_o}=6.0$ (upper panel Fig. S1b). The addition of the small synthesis and degradation terms in E_o (with rate constants k_{13} and k_{14}) keep the autocatalytic E_o -levels sufficiently high such that E_o concentration in the autocatalytic controllers

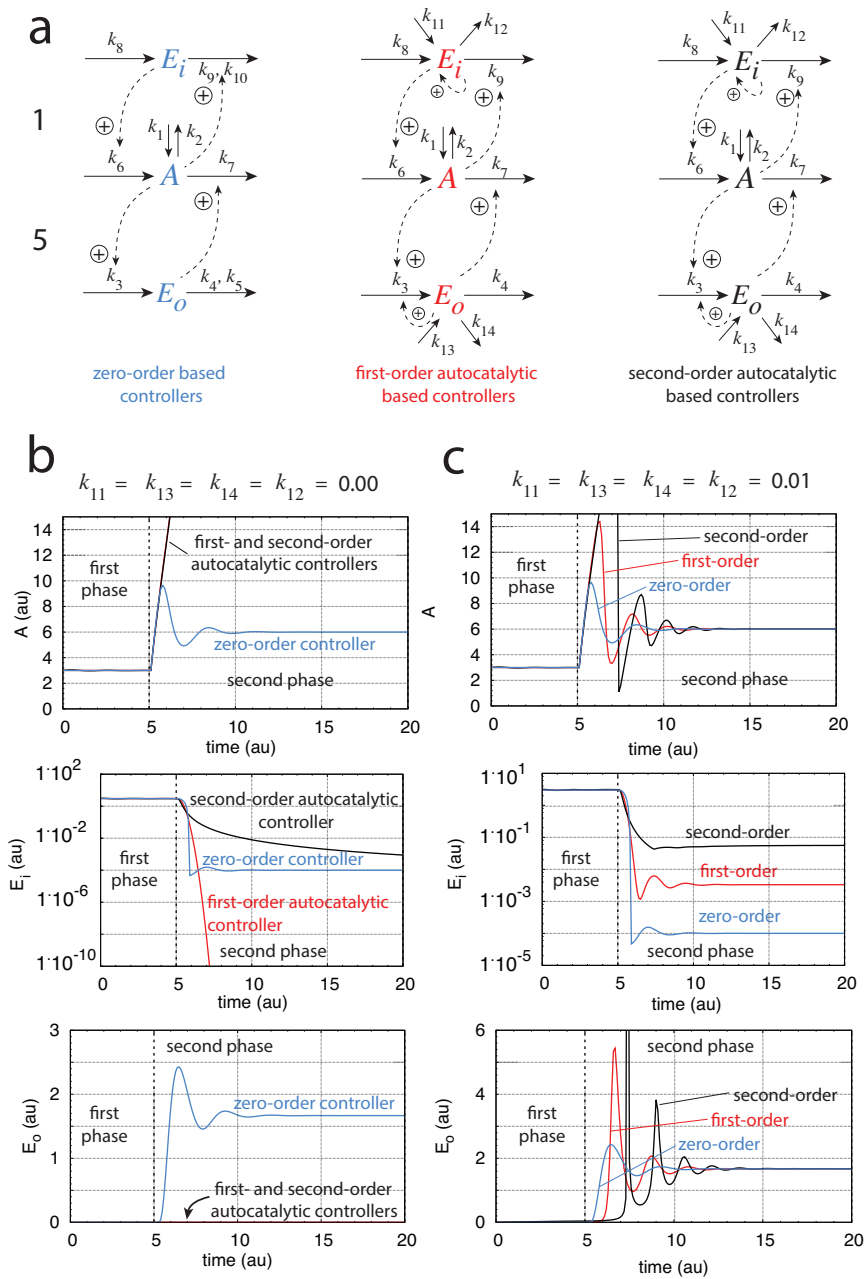


Figure S1: Combined inflow and outflow controllers 1 and 5 with three different implementations of integral control.

can increase and move A to their set-points (Fig. S1c).

Rate equations for combined zero-order controllers (Fig. S1a, left panel, components outlined in blue)

$$\dot{A} = k_1 - k_2 \cdot A + k_6 \cdot E_i - k_7 \cdot A \cdot E_o \quad (\text{S1})$$

$$\dot{E}_i = k_8 - \frac{k_9 \cdot A \cdot E_i}{k_{10} + E_i} \quad (\text{S2})$$

$$\dot{E}_o = k_3 \cdot A - \frac{k_4 \cdot E_o}{k_5 + E_o} \quad (\text{S3})$$

Rate equations for combined first-order autocatalytic controllers (Fig. S1a, middle panel, components outlined in red)

$$\dot{A} = k_1 - k_2 \cdot A + k_6 \cdot E_i - k_7 \cdot A \cdot E_o \quad (\text{S4})$$

$$\dot{E}_i = k_{11} - k_{12} \cdot E_i + k_8 \cdot E_i - k_9 \cdot A \cdot E_i \quad (\text{S5})$$

$$\dot{E}_o = k_{13} - k_{14} \cdot E_o + k_3 \cdot A \cdot E_o - k_4 \cdot E_o \quad (\text{S6})$$

Rate equations for combined second-order autocatalytic controllers (Fig. S1a, right panel, components outlined in black)

$$\dot{A} = k_1 - k_2 \cdot A + k_6 \cdot E_i - k_7 \cdot A \cdot E_o \quad (\text{S7})$$

$$\dot{E}_i = k_{11} - k_{12} \cdot E_i + k_8 \cdot E_i^2 - k_9 \cdot A \cdot E_i^2 \quad (\text{S8})$$

$$\dot{E}_o = k_{13} - k_{14} \cdot E_o + k_3 \cdot A \cdot E_o^2 - k_4 \cdot E_o^2 \quad (\text{S9})$$

Rate constants and initial concentrations (Fig. S1b and Fig. S1c)

The following rate constant values (in au) were used for all three type of controllers: k_1, k_2 , see text; $k_3 = 1.0$, $k_4 = 6.0$, $k_5 = 1 \times 10^{-4}$, $k_6 = k_7 = 1.0$, $k_8 = 3.0$, $k_9 = 1.0$, $k_{10} = 1 \times 10^{-4}$. The values of $k_{11} - k_{14}$ are specified in Fig. S1.

Initial concentrations, combined zero-order controllers: $A_0 = 3.0$, $E_{o,0} = 0.0$, $E_{i,0} = 3.0$. Initial concentrations, combined first-order controllers: $A_0 = 3.0$, $E_{o,0} = 0.0$, $E_{i,0} = 3.01$. Initial concentrations, combined second-order controllers: $A_0 = 3.0$, $E_{o,0} = 0.0$, $E_{i,0} = 3.17$.

References

- [1] Saunders, P. T.; Koeslag, J. H.; Wessels, J. A. *Journal of Theoretical Biology* **1998**, *194*, 163–173.
- [2] Solé, R.; Goodwin, B. *How Complexity Pervades Biology*, *ch.4*; Basic Books, 2000.

Supporting Information 2

Comparing Stationary and Numerical Solutions of A with the Different Implementations of Integral Control for Motif 5

Zero-order Implementation of Integral Control

The rate equations for the zero-order implementation of integral control for motif 5 are:

$$\dot{A} = k_1 - k_2 \cdot A + k_6 - k_7 \cdot A \cdot E_o \quad (\text{S10})$$

$$\dot{E}_o = k_{13} - k_{14} \cdot E_o + k_3 \cdot A - \frac{k_4 \cdot E_o}{k_5 + E_o} \quad (\text{S11})$$

Taking the double derivative of A with respect to time and assuming that $\dot{k}_1 \neq 0$ and $\dot{E}_o \neq 0$, while \dot{A} and \ddot{A} are zero, we get

$$\ddot{A} = \dot{k}_1 - k_2 \cdot \dot{A} - k_7 \cdot \dot{A} \cdot E_o - k_7 \cdot A \cdot \dot{E}_o = \dot{k}_1 - k_7 \cdot A \cdot \dot{E}_o \quad (\text{S12})$$

By setting Eq. S12 to zero the stationary solution A_{ss} is given by:

$$A_{ss} = \frac{\dot{k}_1}{k_7 \cdot \dot{E}_o} \quad (\text{S13})$$

To solve A_{ss} explicitly, Eq. S11 is inserted into Eq. S13, which leads to the following quadratic equation in A_{ss} :

$$k_3 k_7 A_{ss}^2 - k_4 k_7 A_{ss} - \dot{k}_1 = 0 \quad (\text{S14})$$

with the positive solution

$$A_{ss} = \frac{k_4 k_7 + \sqrt{k_7(k_7 + k_4^2 + 4\dot{k}_1 k_3)}}{2k_3 k_7} \quad (\text{S15})$$

which can be rearranged as follows

$$A_{ss} = \frac{1}{2} \cdot \frac{k_4}{k_3} + \sqrt{\frac{k_7^2 k_4^2}{4k_3^2 k_7^2} + \frac{4k_1 k_3 k_7}{4k_3^2 k_7^2}} \quad (\text{S16})$$

Using the expression for the set-point, $A_{set}^{E_o} = k_4/k_3$ (Fig. 2), we finally get

$$A_{ss} = \frac{1}{2} A_{set}^{E_o} + \sqrt{\left(\frac{1}{2} A_{set}^{E_o}\right)^2 + \frac{k_1}{k_3 k_7}} \quad (\text{S17})$$

Autocatalytic Implementation of Integral Control

The stationary solutions for the two autocatalytic implementations of integral control are derived in an analogous manner as for Eq. S17. As an example we use the first-order autocatalytic implementation of integral control. The rate equations for A and E_o are:

$$\dot{A} = k_1 - k_2 \cdot A + k_6 \cdot E_i - k_7 \cdot A \cdot E_o \quad (\text{S18})$$

$$\dot{E}_o = k_{13} - k_{14} \cdot E_o + k_3 \cdot A \cdot E_o - k_4 \cdot E_o \quad (\text{S19})$$

Taking, as above, the double derivative of A with respect to time and assuming that $\dot{k}_1 \neq 0$ and $\dot{E}_o \neq 0$, while \dot{A} and \ddot{A} are zero, we get again Eq. S13. Inserting Eq. S19 into Eq. S13 while assuming that k_{13} and k_{14} are negligible we obtain the following quadratic equation in A_{ss} analogous to Eq. S14:

$$k_3 k_7' A_{ss}^2 - k_4 k_7' A_{ss} - \dot{k}_1 = 0 \quad (\text{S20})$$

where $k_7' = k_7 E_o$. As a result the positive solution of A_{ss} is given as:

$$A_{ss} = \frac{1}{2} A_{set}^{E_o} + \sqrt{\left(\frac{1}{2} A_{set}^{E_o}\right)^2 + \frac{\dot{k}_1}{k_3 k_7 E_o}} \quad (\text{S21})$$

The solution for A_{ss} for the second-order autocatalytic implementation is derived in a similar manner as for Eq. S20, but now with $k_7' = k_7 E_o^2$. The resulting solution for A_{ss} is in this case

$$A_{ss} = \frac{1}{2} A_{set}^{E_o} + \sqrt{\left(\frac{1}{2} A_{set}^{E_o}\right)^2 + \frac{\dot{k}_1}{k_3 k_7 E_o^2}} \quad (\text{S22})$$

Generally, the A_{ss} solution can be written as

$$A_{ss} = \frac{1}{2}A_{set}^{E_o} + \sqrt{\left(\frac{1}{2}A_{set}^{E_o}\right)^2 + \gamma_n} \quad (\text{S23})$$

where γ_n is

$$\gamma_n = \frac{\dot{k}_1}{k_3 k_7 E_o^n} \quad (\text{S24})$$

with $n = 0, 1, 2$ for the zero-, first- and second-order reactions, respectively.

Rate Constants and Initial Concentrations

The following rate constant values (in au) were used for all three type of controllers: for k_1 changes, see legend of Figs. 3; $k_2 = 0.0$, $k_3 = 1.0$, $k_4 = 6.0$, $k_5 = 1 \times 10^{-4}$, $k_6 = k_7 = 5.0$, $k_{13}=k_{14} = 1 \times 10^{-3}$.

Initial concentrations for all three controllers: $A_0 = 6.0$, $E_{o,0} = 0.2$.

Comparing Stationary and Numerical Solutions of A

In the following we compare the derived stationary solutions A_{ss} with the numerical results of A from Fig. 3.

Linear Increase of k_1 with Time

Fig. S2 shows the results when k_1 increases linearly (panel a). In panel b the concentrations of A and A_{ss} of the zero-order controller are shown on the left ordinate, while the right ordinate shows the values of γ_0 . After the onset of the linear increase of k_1 at $t=t_p=2.0$, the stationary solution A_{ss} and the numerical solution A merge after a few time units. This shows that the observed offset of A from $A_{set}^{E_o}=6.0$ is due to the constant term γ_0 and in agreement with Eq. S17. Although the zero-order implementation of integral control is able to counterbalance a linear increase in k_1 , this takes a certain

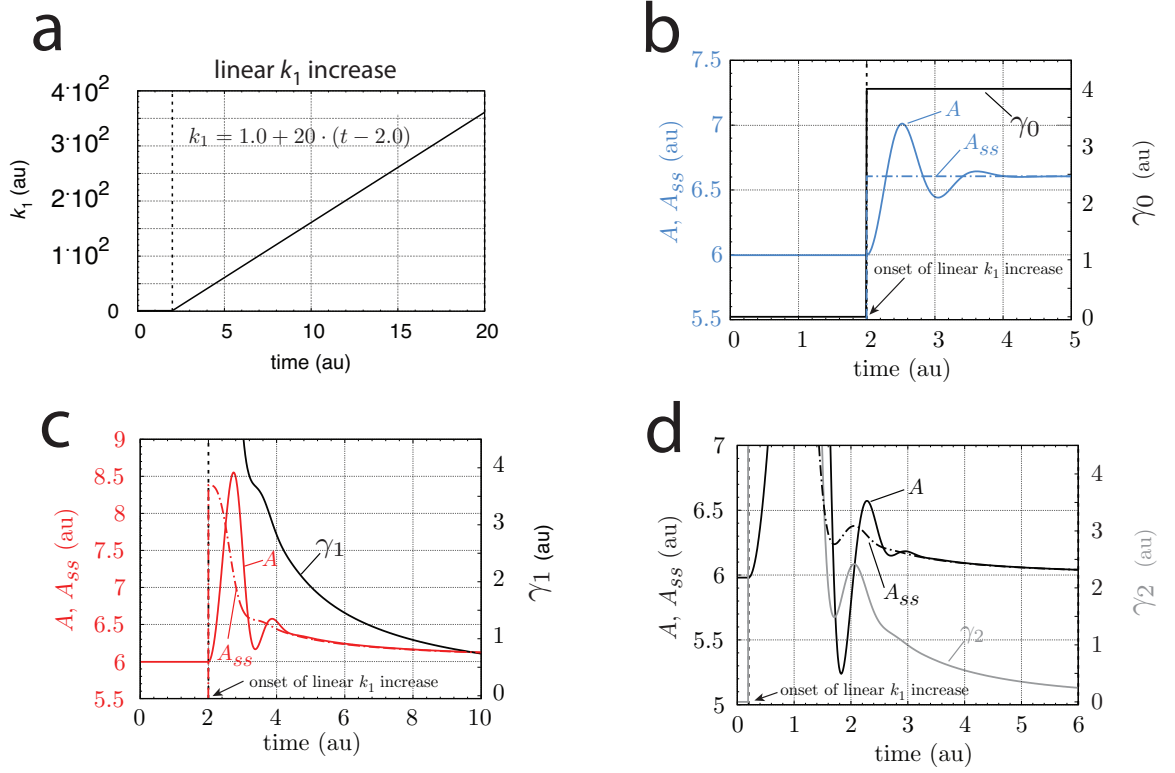


Figure S2: The performance of the three different integral control implementations in motif 5 when k_1 increases linearly with time. (a) k_1 dependence as a function of time. (b) A , A_{ss} , and γ_0 as a function of time for the zero-order implementation of integral control. (c) A , A_{ss} , and γ_1 as a function of time for the first-order autocatalytic implementation of integral control. (d) A , A_{ss} , and γ_2 as a function of time for the second-order autocatalytic implementation of integral control.

time to do so. Once the balance is achieved, the actual A -concentration is off its set-point. The zero-order based controller is not able to reduce this offset, because it has not the capacity to increase the rate removal in A by its compensating flux $j_7=k_6E_o$ beyond a pure first-order dependency in E_o . However, the first-and second-order autocatalytic implementations of integral control have this capacity. Although the compensatory fluxes j_7 for the autocatalytic controllers are formally still first-order with respect to E_o , the underlying first- or second-order autocatalysis in E_o allows an increase in j_7 in order to meet the set-point. In panels c and d it is seen that the decrease of the offset using the autocatalytic controllers is given by the term γ_n (with n being either 1 or 2). The γ_n term decreases as E_o increases with increasing k_1 showing that A is moved precisely to $A_{set}^{E_o}$ when waiting sufficiently long enough.

Exponential Increase of k_1 with Time

Fig. S3 shows the results when k_1 increases exponentially with time (panel a). In panel b the concentrations of A , A_{ss} and the values of γ_0 for the zero-order controller are shown. Note that the controller is not able to defend its homeostatic set-point and A , A_{ss} and γ_0 increase with time. In panel c the behavior for the first-order autocatalytic controller is shown. An offset between A and A_{ss} and $A_{set}^{E_o}$ is observed, which is well described by the stationary solution Eq. S21. Panel d shows the behavior of motif 5 with a second-order autocatalytic implementation of integral control. This controller is able to defend increasing exponential growth in A and keep A at $A_{set}^{E_o}=6.0$.

Hyperbolic Increase of k_1 with Time

Fig. S4 shows the results when k_1 increases hyperbolically with time after a step from $k_1=1.0$ to $k_1=8.0$ (panel a). Although the zero-order and first-order autocatalytic controllers can keep A at its set-point directly after the step, the homeostatic control is lost once k_1 increases too rapidly (panels b and c). The second-order autocatalytic controller is neither able to maintain A at $A_{set}^{E_o}$, although the offset contribution γ_2 is only slightly increasing.

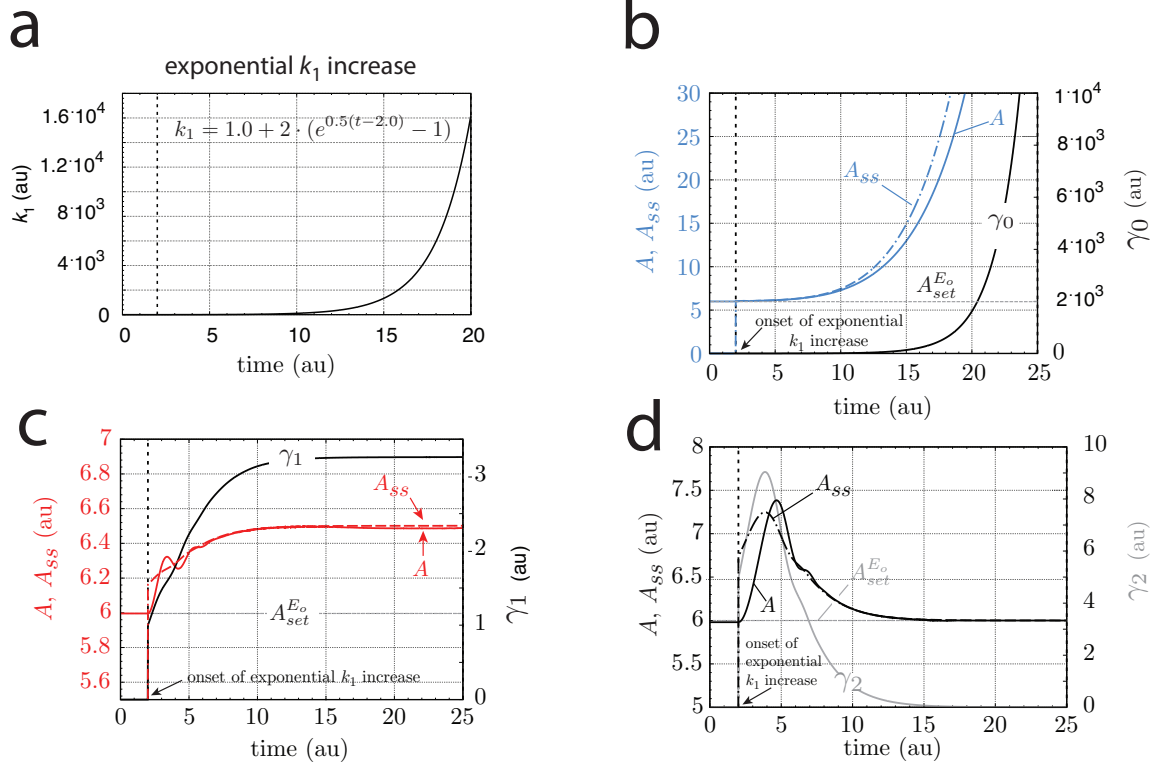


Figure S3: The performance of the three different integral control implementations in motif 5 when k_1 increases exponentially in time. (a) k_1 dependence as a function of time. (b) A , A_{ss} , and γ_0 as a function of time for the zero-order implementation of integral control. (c) A , A_{ss} , and γ_1 as a function of time for the first-order autocatalytic implementation of integral control. (d) A , A_{ss} , and γ_2 as a function of time for the second-order autocatalytic implementation of integral control.

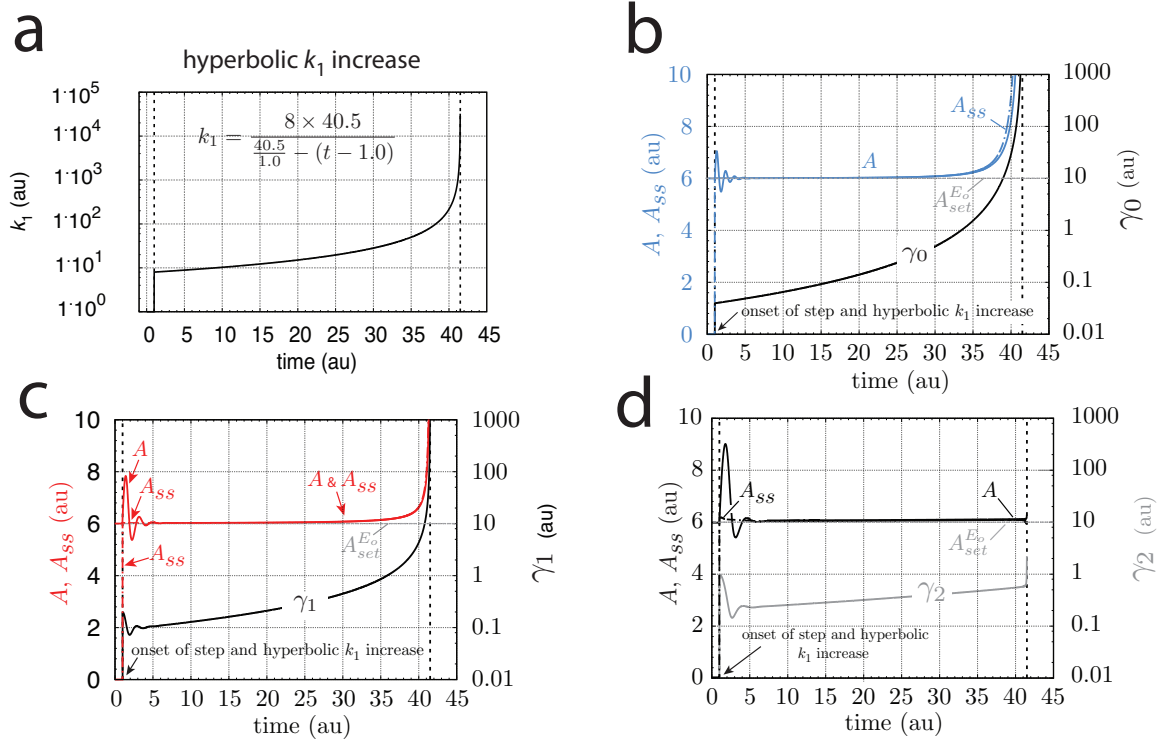


Figure S4: The performance of the three different integral control implementations in motif 5 when k_1 increases hyperbolically with time. (a) k_1 dependence as a function of time. (b) A , A_{ss} , and γ_0 as a function of time for the zero-order implementation of integral control. (c) A , A_{ss} , and γ_1 as a function of time for the first-order autocatalytic implementation of integral control. (d) A , A_{ss} , and γ_2 as a function of time for the second-order autocatalytic implementation of integral control.

Supporting Information 3

Motif 1: Rate Equations for the Three Implementations of Integral Control

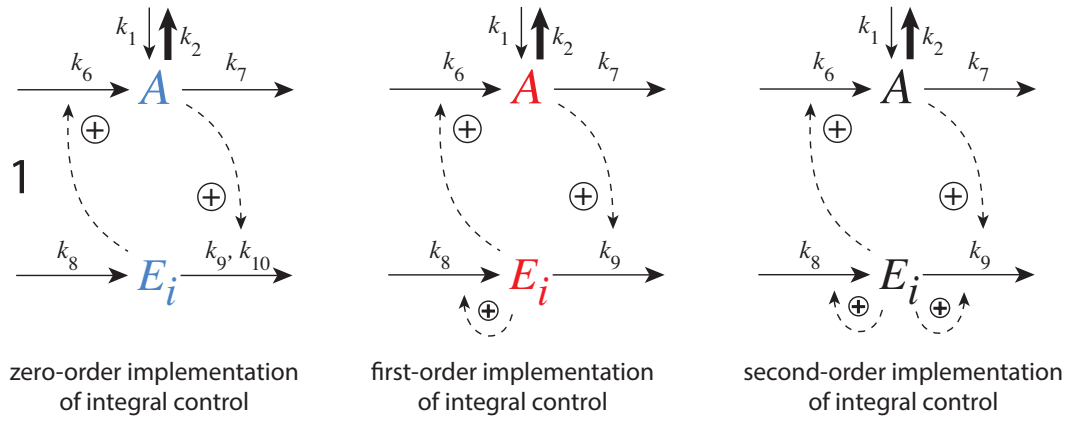


Figure S5: Schematic representations of the three implementations of integral control in motif 1. Components outlined in blue: zero-order type of controller; red: first-order autocatalytic controller; black: second-order autocatalytic controller.

Rate Equations for Zero-Order Controller

$$\dot{A} = k_1 - k_2 \cdot A + k_6 \cdot E_i - k_7 \cdot A \quad (\text{S25})$$

$$\dot{E}_i = k_8 - \left(\frac{k_9 \cdot E_i}{k_{10} + E_i} \right) \cdot A \quad (\text{S26})$$

Setting $\dot{E}_i = 0$ and assuming $k_{10} \ll E_i$ (ideal conditions), the set-point of A , $A_{set}^{E_i}$, at constant k_1/k_2 values, is given by

$$A_{set}^{E_i} = \frac{k_8}{k_9} \quad (\text{S27})$$

Rate Equations for First-Order Controller

$$\dot{A} = k_1 - k_2 \cdot A + k_6 \cdot E_i - k_7 \cdot A \quad (\text{S28})$$

$$\dot{E}_i = k_8 \cdot E_i - k_9 \cdot E_i \cdot A \quad (\text{S29})$$

Setting $\dot{E}_i = 0$ and assuming that $E_i \neq 0$, the set-point of A is given by

$$A_{set}^{E_i} = \frac{k_8}{k_9} \quad (\text{S30})$$

Rate Equations for Second-Order Controller

$$\dot{A} = k_1 - k_2 \cdot A + k_6 \cdot E_i - k_7 \cdot A \quad (\text{S31})$$

$$\dot{E}_i = k_8 \cdot E_i^2 - k_9 \cdot E_i^2 \cdot A \quad (\text{S32})$$

Setting $\dot{E}_i = 0$ and assuming that $E_i \neq 0$, the set-point of A is given by

$$A_{set}^{E_i} = \frac{k_8}{k_9} \quad (\text{S33})$$

Overview of the Performance of the Controllers

Fig. S6 gives an overview of the performances of controller motif 1 with the three implementations of integral control (Fig. S5).

Rate Constants and Initial Concentrations

The following rate constants (in au) and initial concentrations were used for all three types of controllers: $k_1=0.0$, k_2 , see Fig. S6, $k_6=k_7=5.0$, $k_8=3.0$, $k_9=1.0$, $k_{10}=1 \times 10^{-4}$. Initial concentrations: $A_0=3.0$, $E_{o,0}=3.6$.

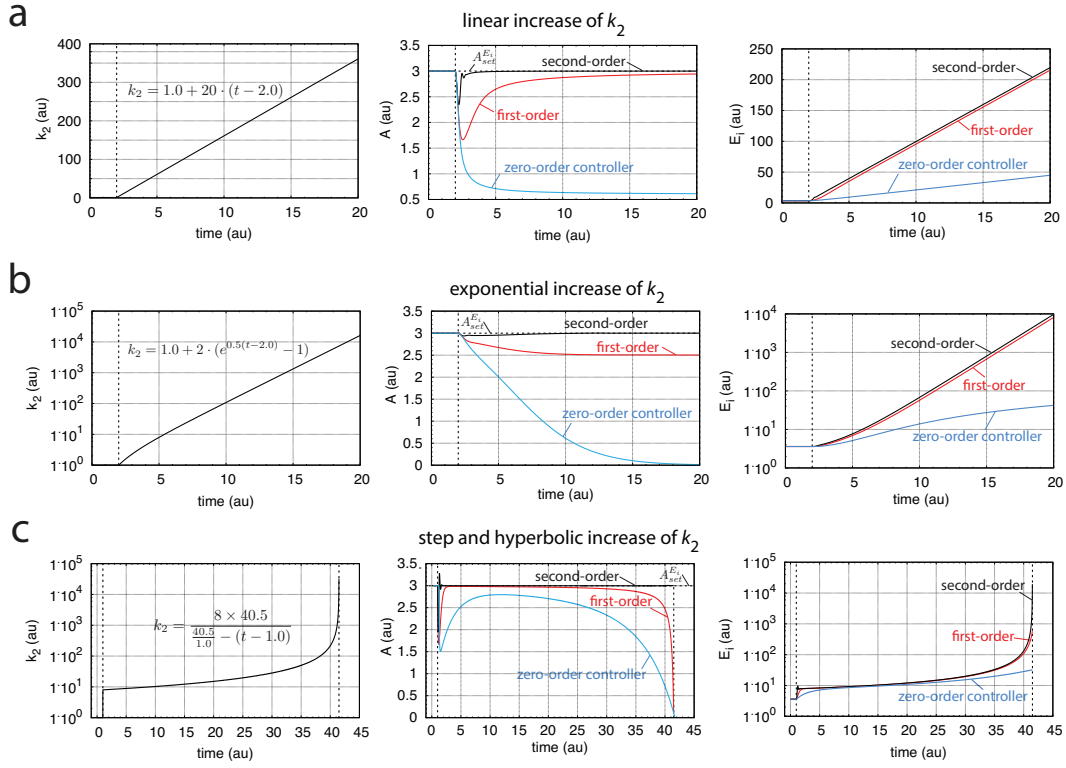


Figure S6: Performance of the three implementations of integral control for controller motif 1 when k_2 increases (a) linearly, (b) exponentially, and (c) hyperbolically.

Stationary Solutions A_{ss} of Motif 1

Zero-order Implementation of Integral Control

Calculating \ddot{A} from Eq. S25 by assuming that all rate constants except k_2 are time independent gives

$$\ddot{A} = -\dot{k}_2 \cdot A - k_2 \cdot \dot{A} + k_6 \cdot \dot{E}_i - k_7 \cdot \dot{A} \quad (\text{S34})$$

Assuming further that $\ddot{A} = \dot{A} = 0$, we get

$$\dot{k}_2 \cdot A_{ss} = k_6 \cdot \dot{E}_i \quad (\text{S35})$$

Inserting Eq. S26 into Eq. S35 and considering ideal zero-order conditions, i.e., $k_{10} \ll E_i$ such that $E_i / (k_{10} + E_i) \approx 1$, Eq. S35 reads

$$\dot{k}_2 \cdot A_{ss} = k_6 \cdot (k_8 - k_9 \cdot A_{ss}) \quad (\text{S36})$$

Rearranging Eq. S36 and solving for A_{ss} gives

$$A_{ss} = \frac{k_6 \cdot k_8}{\dot{k}_2 + k_6 \cdot k_9} = \left(\frac{k_8}{k_9} \right) \cdot \frac{1}{1 + \frac{\dot{k}_2}{k_6 \cdot k_9}} \quad (\text{S37})$$

$$\Rightarrow A_{ss} = A_{set}^{E_i} \cdot \frac{1}{1 + \frac{\dot{k}_2}{k_6 \cdot k_9}} \quad (\text{S38})$$

First-order Implementation of Integral Control

Calculating \ddot{A} from Eq. S28 and assuming that $\ddot{A} = \dot{A} = 0$, together with that all rate constants except k_2 are time independent gives identical to Eq. S35 the relationship

$$\dot{k}_2 \cdot A_{ss} = k_6 \cdot \dot{E}_i \quad (\text{S39})$$

Inserting Eq. S29 into Eq. S39 leads to

$$A_{ss}(\dot{k}_2 + k_6 \cdot k_9 \cdot E_i) = k_6 \cdot k_8 \cdot E_i \quad (\text{S40})$$

Rearranging the equation gives

$$A_{ss} = \frac{k_6 \cdot k_8 \cdot E_i}{\dot{k}_2 + k_6 \cdot k_9 \cdot E_i} = \left(\frac{k_8}{k_9} \right) \cdot \frac{1}{1 + \frac{\dot{k}_2}{k_6 \cdot k_9 \cdot E_i}} = A_{set}^{E_i} \cdot \frac{1}{1 + \frac{\dot{k}_2}{k_6 \cdot k_9 \cdot E_i}} \quad (\text{S41})$$

Second-order Implementation of Integral Control

Using the same above procedure as for the zero-order and first-order implementation of integral control the expression for A_{ss} for the second-order controller is given by

$$A_{ss} = A_{set}^{E_i} \cdot \frac{1}{1 + \frac{\dot{k}_2}{k_6 \cdot k_9 \cdot E_i^2}} \quad (\text{S42})$$

By using γ_n as

$$\gamma_n = \frac{\dot{k}_2}{k_6 \cdot k_9 \cdot E_i^n} \quad (\text{S43})$$

where $n = 0, 1, 2$ for zero-, first-, and second-order reaction, respectively, the expression for A_{ss} can be generalized as

$$A_{ss} = A_{set}^{E_i} \cdot \frac{1}{1 + \gamma_n} \quad (\text{S44})$$

Comparison between Stationary Solutions A_{ss} and Numerical Solutions of A for Motif 1

Linear Increase of k_2 with Time

Fig. S7 gives a comparison between A_{ss} and the numerical solutions for all three implementations of integral control in motif 1 when k_2 increases linearly with time. Typically, as indicated by Eq. S38 the zero-order controller shows a constant offset of A below $A_{set}^{E_i}$ due to the constant \dot{k}_2 . On the other hand, the two autocatalytic implementations of integral control allow E_i to grow fast enough such that the terms γ_1 and γ_2 , which contribute to the offsets from $A_{set}^{E_i}$ decrease monotonically and A approaches the stationary states at $A_{set}^{E_i}$.

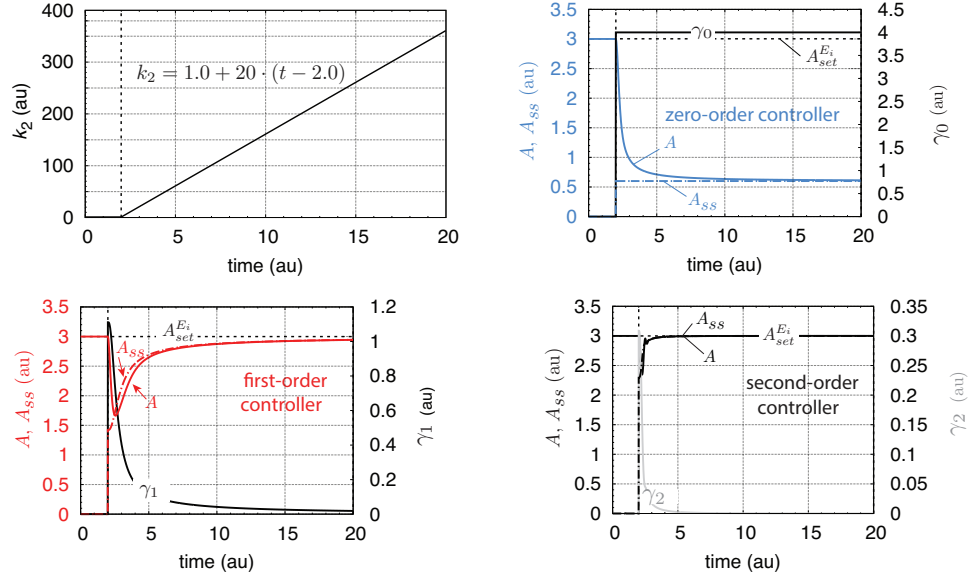
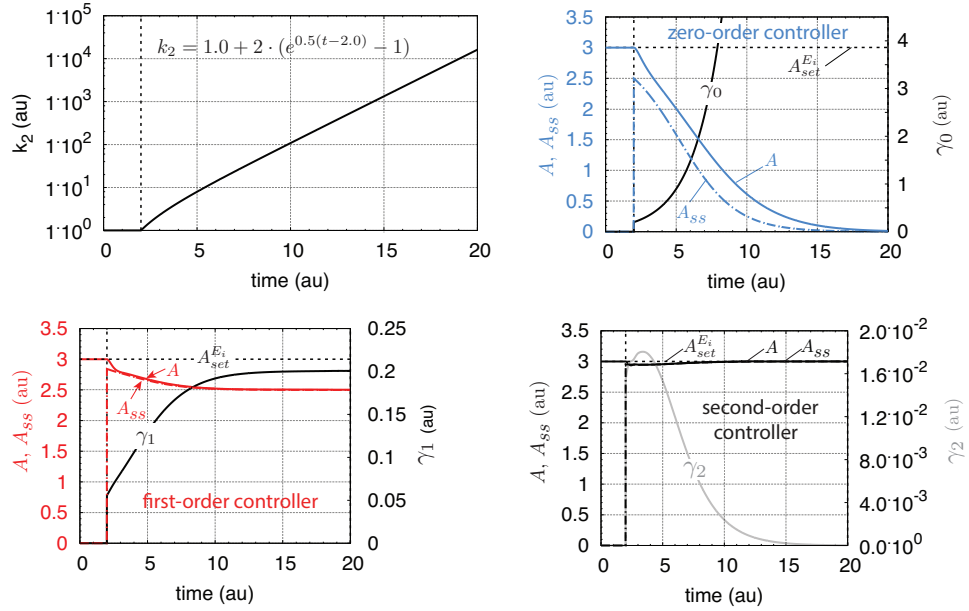


Figure S7: Comparison between stationary solution A_{ss} and numerical solution A and the offset contributions γ_n ($n=0, 1$, and 2) for the three integral control implementations when k_2 increases in a linear fashion with time.

Exponential Increase of k_2 with Time



S17

Figure S8: Comparison between stationary solution A_{ss} and numerical solution A and the offset contributions γ_n ($n=0, 1$, and 2) for the three integral control implementations when k_2 increases exponentially with time.

Fig. S8 gives a comparison between A_{ss} and the numerical solutions for all three implementations of integral control in motif 1 when k_2 increases exponentially with time. The zero-order controller shows a complete breakdown as it is impossible for the controller to counteract the exponential increase of k_2 . The first-order autocatalytic controller is able to counteract, but since this controller is not able to increase E_i faster than k_2 , γ_1 goes to a constant value and the controller shows a steady state in A below $A_{set}^{E_i}$. Only the second-order autocatalytic implementation of integral control allows to compensate for the exponential increase of k_2 and keeps A at $A_{set}^{E_i}$.

Hyperbolic Increase of k_2 with Time

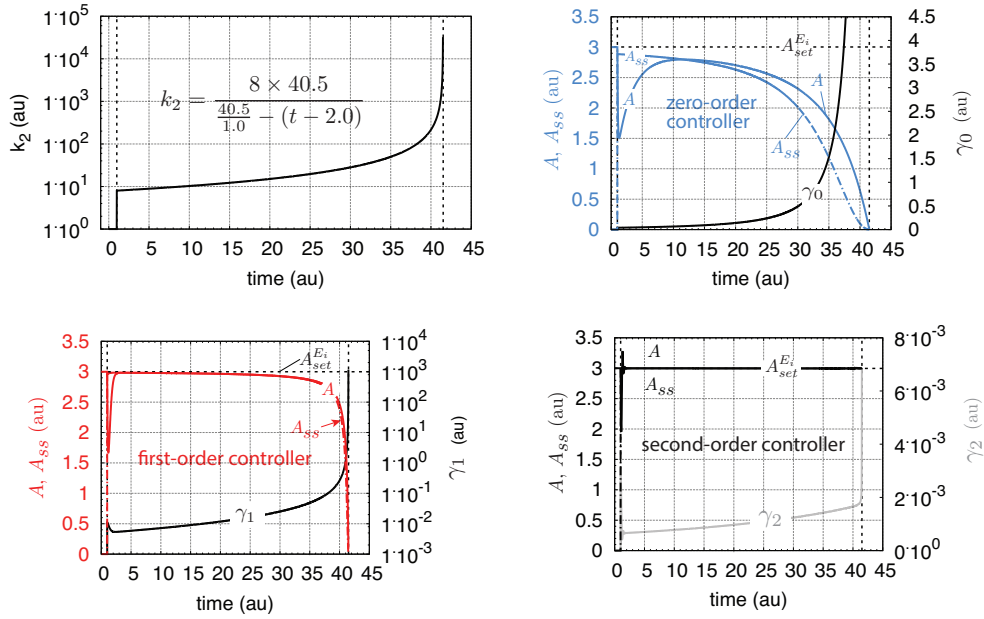


Figure S9: Comparison between stationary solution A_{ss} and numerical solution A and the offset contributions γ_n ($n=0, 1$, and 2) for the three integral control implementations when k_2 increases hyperbolically with time.

Fig. S9 gives a comparison between A_{ss} and the numerical solutions for all three implementations of integral control in motif 1 when k_2 increases

hyperbolically with time. Only the second-order autocatalytic controller allows to keep A close to $A_{set}^{E_i}$. At the end of the simulation time at 41.5 time units $\dot{k}_2=3.24\times 10^6$ while γ_2 has a value of 6.85×10^{-3} indicating a relative deviation of A from $A_{set}^{E_i}$ of about 0.7%.

Supporting Information 4

Motif 2: Rate Equations for the Three Implementations of Integral Control

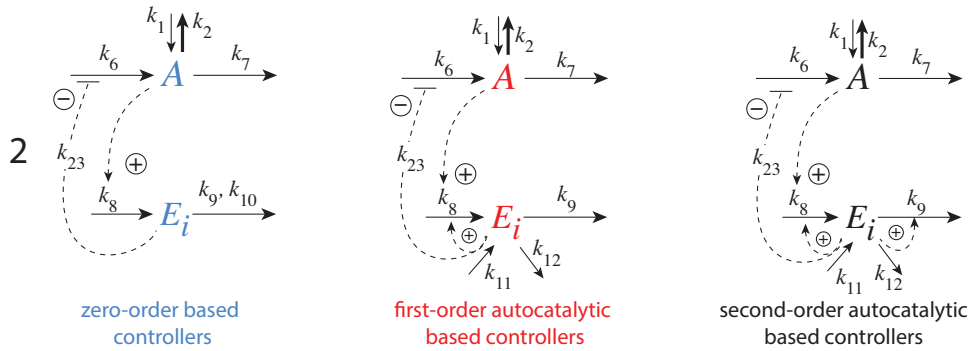


Figure S10: Schematic representations of the three implementations of integral control in motif 2. Components outlined in blue: zero-order type of controller; red: first-order autocatalytic controller; black: second-order autocatalytic controller.

Comparing Stationary and Numerical Solutions of A with the Different Implementations of Integral Control for Motif 2

Rate equations for zero-order controller motif 2

$$\dot{A} = k_1 - k_2 \cdot A + \frac{k_6 \cdot k_{23}}{k_{23} + E_i} - k_7 \cdot A \quad (\text{S45})$$

$$\dot{E}_i = k_8 \cdot A - \frac{k_9 \cdot E_i}{k_{10} + E_i} \quad (\text{S46})$$

The set-point for the controller is calculated by setting Eq. S46 to zero and assuming that $k_{10} \ll E_i$, which leads to the condition $E_i/(k_{10} + E_i) = 1$. Solving for A_{ss} gives the set-point as

$$A_{set}^{E_i} = A_{ss} = \frac{k_9}{k_8} \quad (\text{S47})$$

Rate equations for first-order autocatalytic controller motif 2

$$\dot{A} = k_1 - k_2 \cdot A + \frac{k_6 \cdot k_{23}}{k_{23} + E_i} - k_7 \cdot A \quad (\text{S48})$$

$$\dot{E}_i = k_{11} - k_{12} \cdot E_i + k_8 \cdot A \cdot E_i - k_9 \cdot E_i \quad (\text{S49})$$

Neglecting the contributions of k_{11} and k_{12} to the basal level of E_i , the set-point for this controller is calculated by setting Eq. S49 to zero and solving for A_{ss} under the assumption that the concentration of $E_i \neq 0$, i.e.,

$$E_i \cdot (k_8 A_{ss} - k_9) = 0 \quad \Rightarrow \quad A_{set}^{E_i} = A_{ss} = \frac{k_9}{k_8} \quad (\text{S50})$$

Rate equations for second-order autocatalytic controller motif 2

$$\dot{A} = k_1 - k_2 \cdot A + \frac{k_6 \cdot k_{23}}{k_{23} + E_i} - k_7 \cdot A \quad (\text{S51})$$

$$\dot{E}_i = k_{11} - k_{12} \cdot E_i + k_8 \cdot A \cdot E_i^2 - k_9 \cdot E_i^2 \quad (\text{S52})$$

Setting Eq. S52 to zero and making the same assumptions as in the previous section the set-point of this controller is calculated as

$$E_i^2 \cdot (k_8 A_{ss} - k_9) = 0 \quad \Rightarrow \quad A_{set}^{E_i} = A_{ss} = \frac{k_9}{k_8} \quad (\text{S53})$$

Rate constants and initial concentrations (Fig. 6)

The following rate constant values (in au) were used for all three type of controllers: $k_1 = 1.0$; k_2 , see Fig. 5; $k_6 = 1 \times 10^6$, $k_7 = 10.0$, $k_8 = 16.0$, $k_9 = 96.0$, $k_{10} = 1 \times 10^{-4}$, $k_{11} = k_{12} = k_{23} = 1 \times 10^{-3}$.

Initial concentrations for all three controllers: $A_o = 6.0$, $E_i = 15.4$.

Stationary Solutions for Controller Motif 2

By taking the double derivative of A with respect to time and assuming that $k_2 \neq 0$ and $\dot{E}_i \neq 0$ while \dot{A} and \ddot{A} are zero, we get

$$\ddot{A} = -\dot{k}_2 \cdot A - \frac{k_6 \cdot k_{23}}{(k_{23} + E_i)^2} \dot{E}_i = 0 \quad (\text{S54})$$

To get A_{ss} for the zero-order controller, Eq. S46 is inserted into Eq. S54 under the assumption that $k_{10} \ll E_i$, i.e., $k_9 E_i / (k_{10} + E_i) = k_9$ leading to

$$-\dot{k}_2 A_{ss} - \frac{k_6 k_{23}}{(k_{23} + E_i)^2} (k_8 A_{ss} - k_9) = 0 \quad (\text{S55})$$

Observing that $A_{set}^{E_i} = k_9 / k_8$, Eq. S55 can be rearranged to

$$A_{ss} = -\frac{k_6 k_8 k_{23}}{\dot{k}_2 (k_{23} + E_i)^2} (A_{ss} - A_{set}^{E_i}) \quad (\text{S56})$$

Using γ_0 as

$$\gamma_0 = \frac{k_6 k_8 k_{23}}{\dot{k}_2 (k_{23} + E_i)^2} \quad (\text{S57})$$

A_{ss} for the zero-order type of controller can be written as

$$A_{ss} = A_{set}^{E_i} \left(\frac{\gamma_0}{1 + \gamma_0} \right) \quad (\text{S58})$$

An analogous expression for A_{ss} can be derived for the autocatalytic controllers. The resulting A_{ss} expressions for all controllers can be summarized as follows

$$A_{ss} = A_{set}^{E_i} \left(\frac{\gamma_n}{1 + \gamma_n} \right) \quad (\text{S59})$$

where

$$\gamma_n = \frac{k_6 k_8 k_{23} E_i^n}{k_2 (k_{23} + E_i)^2} \quad (\text{S60})$$

with $n = 0, 1$, and 2 for the zero-, first- and second-order controllers, respectively.

The γ values of the three controllers are an indicator how the different controllers perform. When $\gamma_n \gg 1$, the offset/error between A and $A_{set}^{E_i}$ is low, while when $\gamma_n \ll 1$ the controller performance is poor.

Comparing Stationary and Numerical Solutions of A

Linear Increase of k_2 with Time

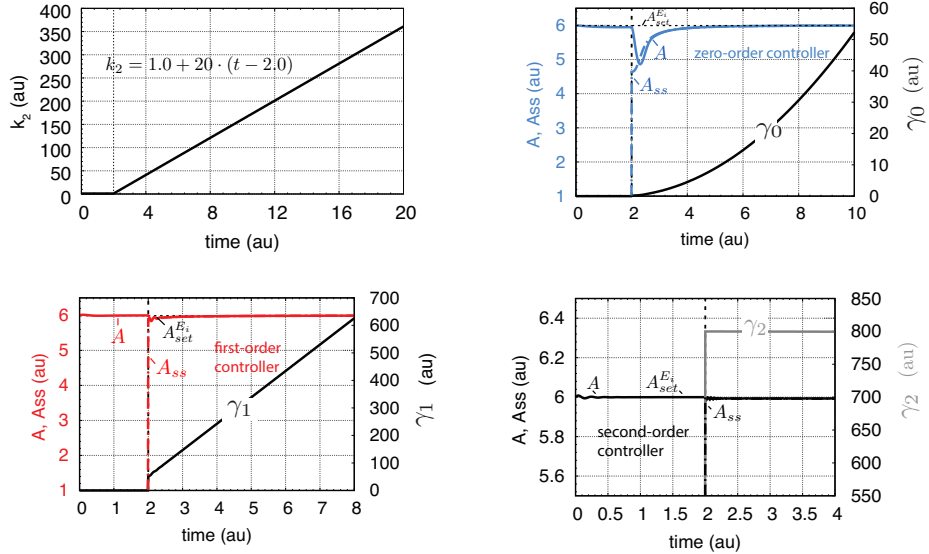


Figure S11: Comparison between stationary solution A_{ss} and numerical solution A and the offset contributions γ_n for the three integral control implementations in motif 2 when k_2 increases linearly.

Fig. S11 shows the A_{ss} and numerical A values for the motif 2 controllers when k_2 increases linearly with time. The zero- and first-order type of con-

trollers have their A concentrations close to their set-points and show increasing γ values with time, i.e., reducing the error between A_{ss} and $A_{set}^{E_i}$.

Exponential Increase of k_2 with Time

During the exponential increase of k_2 the controllers' A_{ss} is close to the set-point due to their large γ values. However, for the two autocatalytic controllers the γ values rapidly decrease. When the γ 's reach zero the controllers break down. Only the zero-order type of controller shows a temporary increase of γ_0 . As the concentration of E_i becomes low E_i cannot maintain the functionality of the negative feedback loop and the zero-order controller breaks down (see Fig. 5b, right panel). As a result, the γ_0 value decreases (Fig. S12). For the second-order autocatalytic controller the break-down starts to occur already at about 15 time units, due to the low γ_2 value while this controller's E_i value is still relatively high.

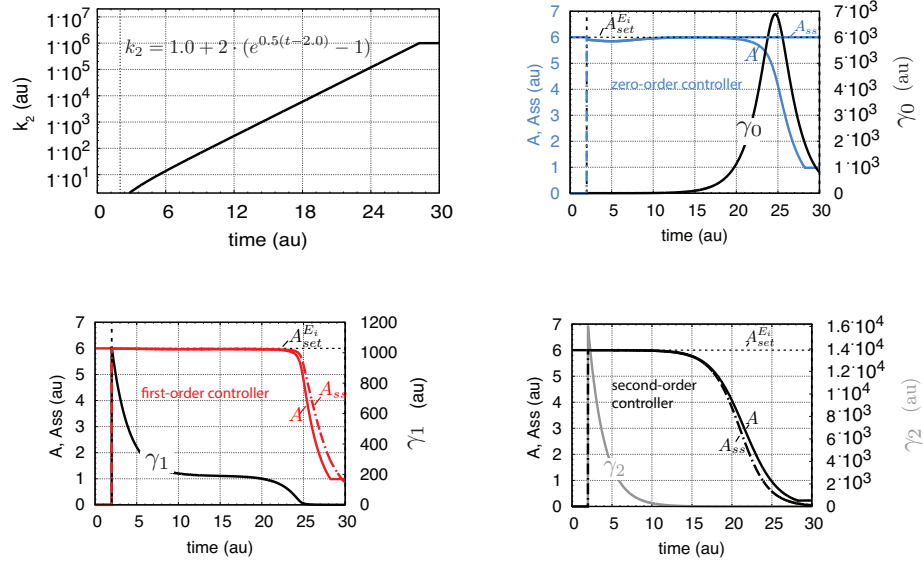


Figure S12: Comparison between stationary solution A_{ss} and numerical solution A and the offset contributions γ_n for the three integral control implementations in motif 2 when k_2 increases exponentially.

Hyperbolic Increase of k_2 with Time

The k_2 undergoes at the start of the second phase a jump from 1 to 8 and then increases hyperbolically. Initially, the hyperbolic increase is relatively slow and the controllers are able to adapt after the k_2 -jump to the slowly increasing k_2 , indicated by the relative high (but decreasing) γ values.

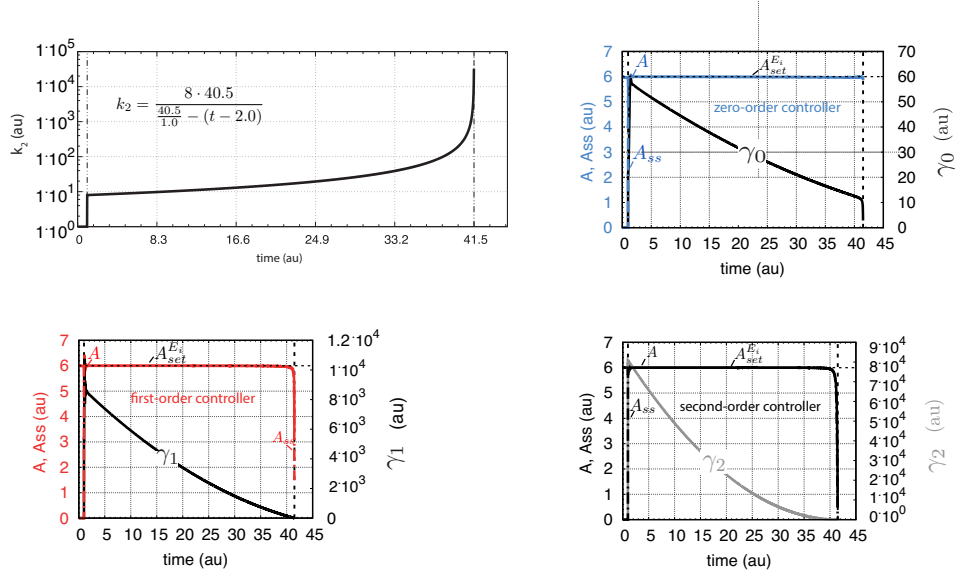


Figure S13: Comparison between stationary solution A_{ss} and numerical solution A and the offset contributions γ_n for the three integral control implementations in motif 2 when k_2 increases hyperbolically.

The zero-order controller performs best and is able to hold its A value close to $A_{set}^{E_i}$ for the longest time (see Fig. 5c, middle panel).

Supporting Information 5

Comparing Stationary and Numerical Solutions of A with the Different Implementations of Integral Control for Motif 6

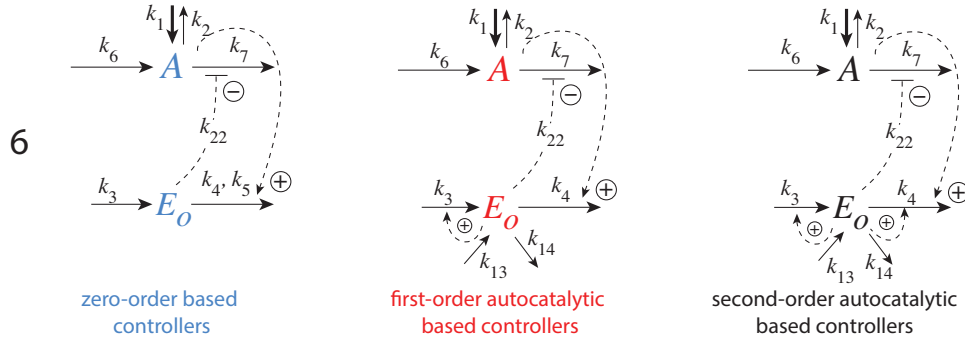


Figure S14: Schematic representations of the three implementations of integral control in motif 6. Components outlined in blue: zero-order type of controller; red: first-order autocatalytic controller; black: second-order autocatalytic controller.

Zero-order Implementation of Integral Control

$$\dot{A} = k_1 - k_2 \cdot A + k_6 - \frac{k_7 \cdot k_{22} \cdot A}{(k_{22} + E_o)} \quad (\text{S61})$$

$$\dot{E}_o = k_3 - \frac{k_4 \cdot E_o \cdot A}{k_5 + E_o} \quad (\text{S62})$$

The set-point of the zero-order type of controller is calculated by assuming that $k_5 \ll E_o$ (ideal conditions) such that $E_o/(k_5 + E_o) = 1$. Setting then Eq. S62 to zero gives

$$A_{set}^{E_o} = A_{ss} = \frac{k_3}{k_4} \quad (\text{S63})$$

To calculate A_{ss} for changing k_1 values we take the double derivative of A with respect to time and assume that $\dot{k}_1 \neq 0$ and $\dot{E}_o \neq 0$, while \dot{A} and \ddot{A} are zero, i.e.,

$$\ddot{A} = \dot{k}_1 + \frac{k_7 \cdot k_{22} \cdot A_{ss}}{(k_{22} + E_o)^2} \dot{E}_o = 0 \quad (\text{S64})$$

By inserting Eq. S62 into Eq. S64 under the assumption that $E_o/(k_5 + E_o) = 1$ and setting the resulting equation to 0 we get

$$\dot{k}_1 + \frac{k_3 \cdot k_7 \cdot k_{22} \cdot A_{ss}}{(k_{22} + E_o)^2} - \frac{k_4 \cdot k_7 \cdot k_{22} \cdot A_{ss}^2}{(k_{22} + E_o)^2} = 0 \quad (\text{S65})$$

which can be written in a quadratic form as

$$A_{ss}^2 - A_{ss} \left(\frac{k_3}{k_4} \right) - \frac{\dot{k}_1 \cdot (k_{22} + E_o)^2}{k_4 \cdot k_7 \cdot k_{22}} = 0 \quad (\text{S66})$$

Using $A_{set}^{E_o} = \frac{k_3}{k_4}$ and γ_0 as

$$\gamma_0 = \frac{\dot{k}_1 \cdot (k_{22} + E_o)^2}{k_4 \cdot k_7 \cdot k_{22}} \quad (\text{S67})$$

the stationary solution A_{ss} of the zero-order controller is given by:

$$A_{ss} = \left(\frac{A_{set}^{E_o}}{2} \right) + \sqrt{\left(\frac{A_{set}^{E_o}}{2} \right)^2 + \gamma_0} \quad (\text{S68})$$

Autocatalytic Implementation of Integral Control

The stationary solutions for the two autocatalytic implementations of integral control are derived in an analogous manner as for Eq. S68. As an example we use the first-order autocatalytic implementation of integral control. The rate equations for A and E_o are:

$$\dot{A} = k_1 - k_2 \cdot A + k_6 - \frac{k_7 \cdot k_{22} \cdot A}{(k_{22} + E_o)} \quad (\text{S69})$$

$$\dot{E}_o = k_{13} - k_{14} \cdot E_o + k_3 \cdot E_o - k_4 \cdot E_o \cdot A \quad (\text{S70})$$

By neglecting the contributions of k_{13} and k_{14} in Eq. S70 the set-point $A_{set}^{E_o}$ is calculated as the steady state in A when k_1 and k_2 are constants. By setting Eq. S70 to zero we get

$$E_{o,ss}(k_3 - k_4 \cdot A_{ss}) = 0 \quad \Rightarrow \quad A_{set}^{E_o} = A_{ss} = \frac{k_3}{k_4} \quad (\text{S71})$$

To calculate A_{ss} when k_1 is a function of time the double derivative of A with respect to time is taken and assuming that $\dot{k}_2 \neq 0$ and $\dot{E}_o \neq 0$, while \ddot{A} and \ddot{A} are assumed to be zero. Inserting Eq. S70 (neglecting k_{13} and k_{14}) into Eq. S64 we obtain the following quadratic equation in A_{ss} analogous to Eq. S66:

$$A_{ss}^2 - A_{ss} \left(\frac{k_3}{k_4} \right) - \frac{\dot{k}_1 \cdot (k_{22} + E_o)^2}{k_4 \cdot k_7 \cdot k_{22} \cdot E_o} = 0 \quad (\text{S72})$$

with the solution

$$A_{ss} = \left(\frac{A_{set}^{E_o}}{2} \right) + \sqrt{\left(\frac{A_{set}^{E_o}}{2} \right)^2 + \gamma_1} \quad (\text{S73})$$

where

$$\gamma_1 = \frac{\dot{k}_1 \cdot (k_{22} + E_o)^2}{k_4 \cdot k_7 \cdot k_{22} \cdot E_o} \quad (\text{S74})$$

The generalized solution for all controller types is given as

$$A_{ss} = \left(\frac{A_{set}^{E_o}}{2} \right) + \sqrt{\left(\frac{A_{set}^{E_o}}{2} \right)^2 + \gamma_n} \quad (\text{S75})$$

where

$$\gamma_n = \frac{\dot{k}_1 \cdot (k_{22} + E_o)^2}{k_4 \cdot k_7 \cdot k_{22} \cdot E_o^n} \quad (\text{S76})$$

with $n = 0, 1, 2$ for the zero-, first- and second-order reactions, respectively.

Overview of the Performance of the Controllers

Fig. S15 gives an overview of the performance of controller motif 6 with the three implementations of integral control (Fig. S14).

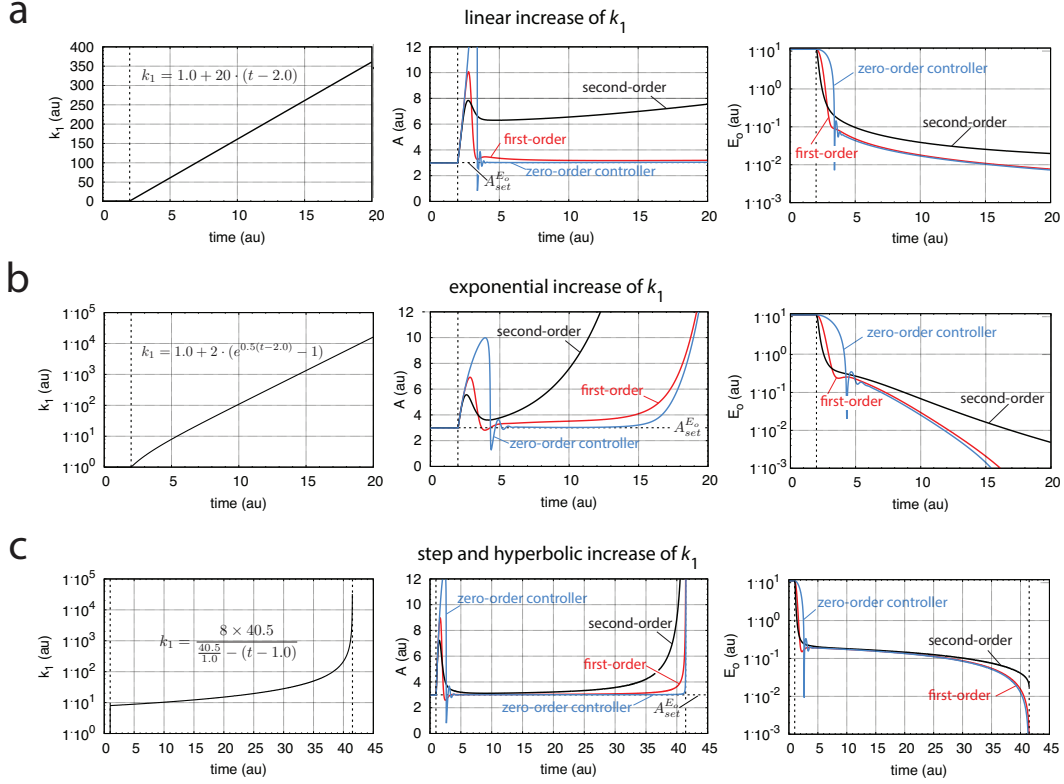


Figure S15: Performance of the three implementations of integral control (Fig. S14) for controller motif 6 when k_1 increases linearly (a, left panel), exponentially (b, left panel), and hyperbolically (c, left panel).

Rate constants and initial concentrations (Fig. S15)

The following rate constant values (in au) were used for all three type of controllers: k_1 , see Fig. S15; $k_2 = 1.0$, $k_3 = 3.0$, $k_4 = 1.0$, $k_5 = 1 \times 10^{-4}$, $k_6 = 1 \times 10^1$, $k_7 = 1 \times 10^3$, $k_{22} = 3 \times 10^{-2}$.

Initial concentrations for all three controllers: $A_0 = 3.0$, $E_{o,0} = 11.2$.

Comparing Stationary and Numerical Solutions of A

Linear Increase of k_1 with Time

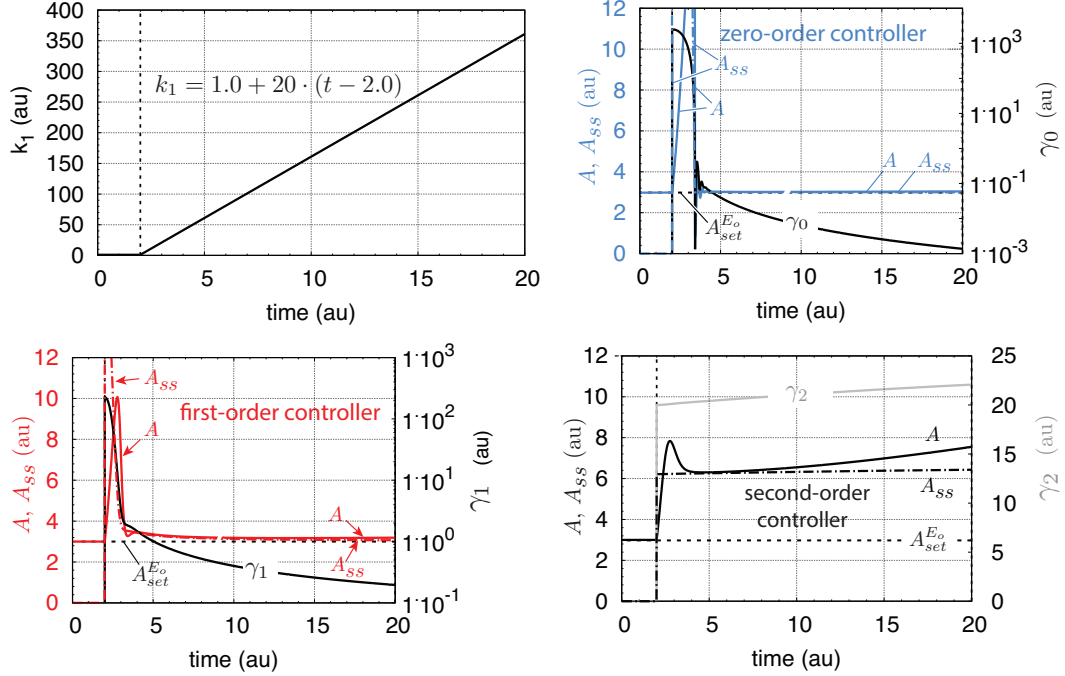


Figure S16: Comparison between stationary solution A_{ss} and numerical solution A and the offset contributions γ_n for the three integral control implementations in motif 6 when k_1 increases linearly with time.

Fig. S16 shows the A_{ss} and numerical A values for the zero-order type of controller 6 when k_1 increases linearly with time. The zero- and first-order type of controllers move their A concentrations close towards their homeostatic set-points as indicated by their decreasing γ_0 and γ_1 values. The second-order autocatalytic controller is not able to defend its homeostatic set-point indicated by the increasing γ_2 with time.

Exponential Increase of k_1 with Time

During the exponential increase of k_1 none of the integral control implementations perform well as indicated by the increase of the respective γ values of the offset contributions. Only the zero-order type of controller shows a temporary approach of A to $A_{set}^{E_o}$ as indicated by the decreasing γ_0 . However, as the concentration of E_o becomes too low to maintain the functionality of the negative feedback loop, the zero-order controller breaks down and γ_0 increases.

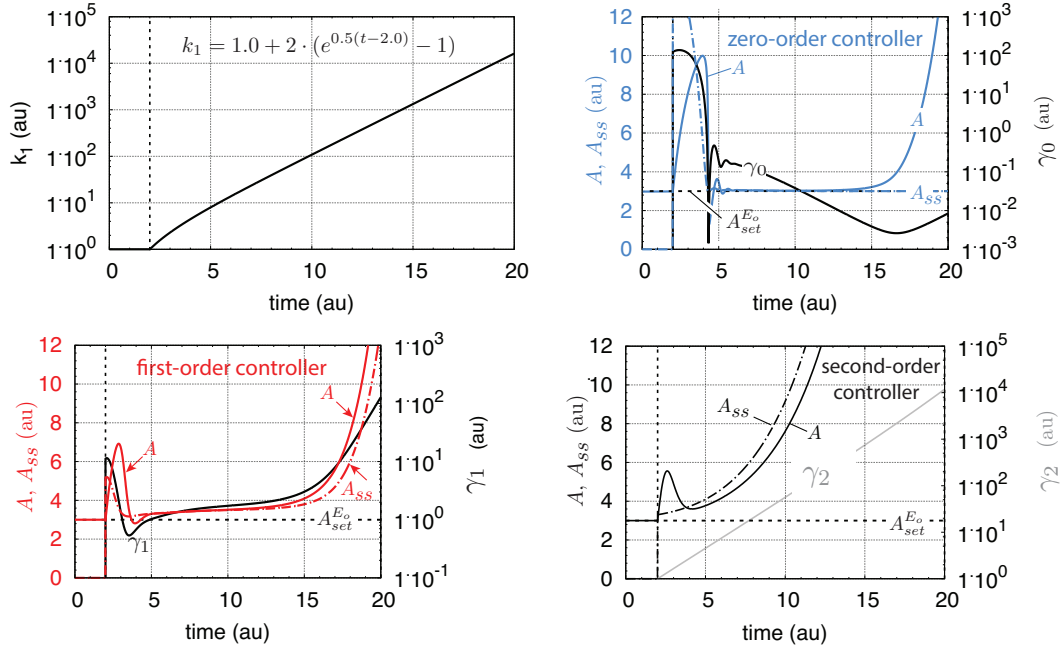


Figure S17: Comparison between stationary and numerical solutions A_{ss} and A together with the offset contributions γ_n for the three integral control implementations in motif 6 when k_1 increases exponentially as a function of time.

Hyperbolic Increase of k_1 with Time

Here k_1 undergoes at the start of the second phase a jump from 1 to 8 and then increases hyperbolically. Initially, the hyperbolic increase is relatively slow and the controllers are able to adapt to the slowly increasing k_1 . The γ values of the three controllers is an indicator how the different controllers perform (Fig. S18). For the zero-order controller γ_0 decreases and indicates that the offset/error between A and $A_{set}^{E_o}$ decreases. However, as k_1 grows rapidly near the border when k_1 reaches infinity, the controller breaks down and A increases rapidly with time.

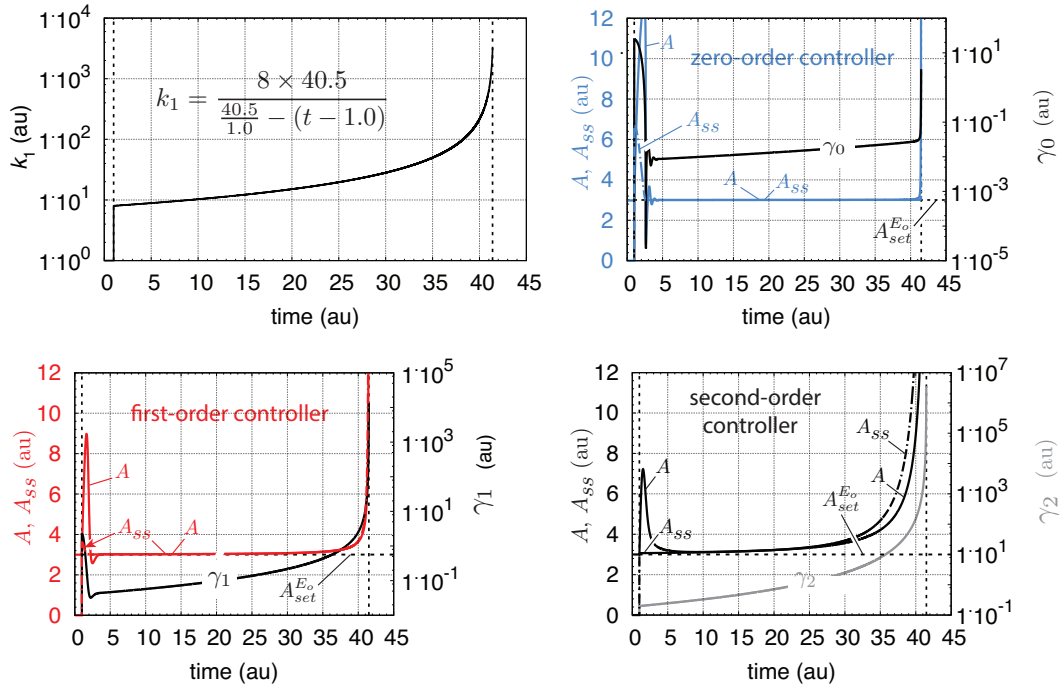


Figure S18: Comparison between stationary solution A_{ss} and numerical solution A and the offset contributions γ_n for the three integral control implementations in motif 6 when k_1 increases hyperbolically with time.

The autocatalytic controllers are able to compensate for the initial k_1 -jump and for the slowly increasing k_1 . As k_1 increases rapidly towards infinity the

autocatalytic controllers are not able to decrease E_o rapidly enough (such as the zero-order controller can) due to their autocatalytic production terms of E_o . Due to its hyperbolic ability to decrease E_o the zero-order controller performs best and is able to hold its A value close to $A_{set}^{E_o}$ for the longest time.

Supporting Information 6

Comparing Stationary and Numerical Solutions of A with the Different Implementations of Integral Control for Motif 3

Fig. S19 indicates the three implementations of integral control in motif 3.

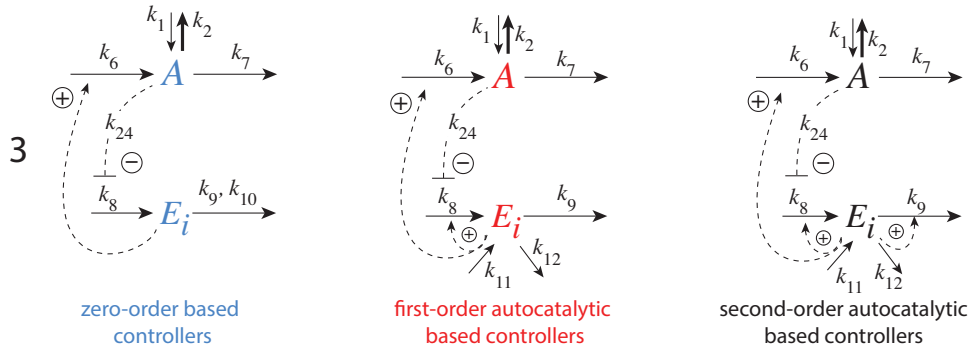


Figure S19: Reaction schemes of motif 3 with three implementations of integral control.

Rate Equations and Set-Point for the Zero-Order Controller

The implementation of integral control by zero-order degradation of E_i has the following rate equations for A and E_i:

$$\dot{A} = k_1 - k_2 \cdot A + k_6 \cdot E_i - k_7 \cdot A \quad (\text{S77})$$

$$\dot{E}_i = \frac{k_8 \cdot k_{24}}{k_{24} + A} - \frac{k_9 \cdot E_i}{k_{10} + E_i} \quad (\text{S78})$$

The set-point $A_{set}^{E_i}$ is calculated for ideal zero-order conditions, i.e., $k_{10} \ll E_i$ such that $E_i/(k_{10}+E_i)=1$. Using these conditions and setting $\dot{E}_i=0$, the set-point is calculated as the steady state value of A , A_{ss} :

$$\dot{E}_i = 0 = \frac{k_8 \cdot k_{24}}{k_{24} + A_{ss}} - k_9 \quad (\text{S79})$$

Solving for A_{ss} gives the set-point:

$$A_{set}^{E_i} = A_{ss} = k_{24} \left(\frac{k_8}{k_9} - 1 \right) \quad (\text{S80})$$

Rate Equations and Set-Point for the First-Order Autocatalytic Controller

When implementing integral control by a first-order autocatalytic reaction in E_i the rate equations are:

$$\dot{A} = k_1 - k_2 \cdot A + k_6 \cdot E_i - k_7 \cdot A \quad (\text{S81})$$

$$\dot{E}_i = k_{11} - k_{12} \cdot E_i + \frac{k_8 \cdot E_i \cdot k_{24}}{k_{24} + A} - k_9 \cdot E_i \quad (\text{S82})$$

The rate constants k_{11} and k_{12} are considered to be small with the purpose to keep E_i at a low nonzero level. In the calculation of the controller's set-point the contributions by k_{11} and k_{12} to E_i are neglected. Using this assumption together with $\dot{E}_i=0$ and $E_i \neq 0$, the set-point is calculated as in the previous section, i.e.

$$\dot{E}_i = 0 = \left(\frac{k_8 \cdot k_{24}}{k_{24} + A_{ss}} - k_9 \right) \cdot E_i \quad (\text{S83})$$

leading to the same set-point

$$A_{set}^{E_i} = A_{ss} = k_{24} \left(\frac{k_8}{k_9} - 1 \right) \quad (\text{S84})$$

as in Eq. S80.

Rate Equations and Set-Point for the Second-Order Autocatalytic Controller

When implementing integral control by a second-order autocatalytic generation of E_i and a second-order degradation with respect to E_i , the rate equations become:

$$\dot{A} = k_1 - k_2 \cdot A + k_6 \cdot E_i - k_7 \cdot A \quad (\text{S85})$$

$$\dot{E}_i = k_{11} - k_{12} \cdot E_i + \frac{k_8 \cdot E_i^2 \cdot k_{24}}{k_{24} + A} - k_9 \cdot E_i^2 \quad (\text{S86})$$

As for the first-order controller the rate constants k_{11} and k_{12} are considered to be small and are neglected in the calculation of the controller's set-point. Assuming $\dot{E}_i=0$ and $E_i \neq 0$, the set-point is calculated as in the previous sections, i.e.

$$\dot{E}_i = 0 = \left(\frac{k_8 \cdot k_{24}}{k_{24} + A_{ss}} - k_9 \right) \cdot E_i^2 \quad (\text{S87})$$

leading to

$$A_{set}^{E_i} = A_{ss} = k_{24} \left(\frac{k_8}{k_9} - 1 \right) \quad (\text{S88})$$

Rate constants and initial concentrations

The following rate constant values (in au) were used for all three type of controllers: $k_1=1.0$, k_2 , see Fig. 7; $k_3=1.0$, $k_4=61.0$, $k_5=1 \times 10^{-7}$, $k_6=10.0$, $k_7=0.0$, $k_8=31.0$, $k_9=1.0$, $k_{11}=k_{12}=1.0 \times 10^{-3}$. The inhibiting constant of E_i synthesis by A is $k_{24}=0.1$.

Initial concentrations for all three controllers: $A_0 = 3.0$, $E_{i,0} = 0.2$.

Stationary Solutions for A using Controller Motif 3

Zero-order Controller

Calculating \ddot{A} from Eq. S77 by assuming that $\ddot{A}=\dot{A}=0$, we get

$$\ddot{A} = -\dot{k}_2 \cdot A - k_1 \dot{A} + k_6 \dot{E}_i \quad (\text{S89})$$

By setting Eq. S89 to zero the stationary solution A_{ss} (when $\dot{k}_2 \neq 0$ and $\dot{E}_i \neq 0$) is given by:

$$A_{ss} = \frac{k_6 \dot{E}_i}{\dot{k}_2} \quad (\text{S90})$$

To solve for A_{ss} , Eq. S78 is inserted into Eq. S90, which leads to the following quadratic equation in A_{ss} :

$$A_{ss}^2 + A_{ss} \left(\frac{k_6 k_9}{\dot{k}_2} + k_{24} \right) - \frac{k_6 k_9}{\dot{k}_2} \cdot A_{set}^{E_i} = 0 \quad (\text{S91})$$

Eq. S91 shows that when $\dot{k}_2=0$ the controller's steady state is at its set-point, i.e., $A_{ss}=A_{set}^{E_i}$. In case $\dot{k}_2 \neq 0$ A_{ss} is

$$A_{ss} = - \left(\frac{\gamma_0 + k_{24}}{2} \right) + \sqrt{\left(\frac{\gamma_0 + k_{24}}{2} \right)^2 + \gamma_0 A_{set}^{E_i}} \quad (\text{S92})$$

where

$$\gamma_0 = \frac{k_6 k_9}{\dot{k}_2} \quad (\text{S93})$$

and

$$A_{set}^{E_i} = k_{24} \left(\frac{k_8}{k_9} - 1 \right) \quad (\text{S94})$$

Autocatalytic Implementation of Integral Control

The stationary solutions for the two autocatalytic implementations of integral control are derived in an analogous manner as for Eq. S92. As an example we use the first-order autocatalytic controller.

Taking, as above, the double derivative of A with respect to time and assuming that $\dot{k}_2 \neq 0$ and $\dot{E}_i \neq 0$, while $\dot{A}=\ddot{A}=0$, we get again Eq. S90. Inserting Eq. S82 into Eq. S90 while assuming that k_{11} and k_{12} are negligible we obtain the following equation in A_{ss} analogous to Eq. S91:

$$A_{ss}^2 + A_{ss} \left(\frac{k_6 k_9 E_i}{\dot{k}_2} + k_{24} \right) - \frac{k_6 k_9 E_i}{\dot{k}_2} \cdot A_{set}^{E_i} = 0 \quad (\text{S95})$$

The quadratic expression of A_{ss} for the first-order autocatalytic implementation is derived in the same way as for the zero-order controller leading to Eq. S95. The solution of A_{ss} for the first-order controller is

$$A_{ss} = - \left(\frac{\gamma_1 + k_{24}}{2} \right) + \sqrt{\left(\frac{\gamma_1 + k_{24}}{2} \right)^2 + \gamma_1 A_{set}^{E_i}} \quad (\text{S96})$$

where

$$\gamma_1 = \frac{k_6 k_9 E_i}{\dot{k}_2} \quad (\text{S97})$$

and the same $A_{set}^{E_i}$ as in Eq. S94.

For the second-order autocatalytic controller we have an analogous solution for A_{ss} as Eq. S96, i.e.

$$A_{ss} = - \left(\frac{\gamma_2 + k_{24}}{2} \right) + \sqrt{\left(\frac{\gamma_2 + k_{24}}{2} \right)^2 + \gamma_2 A_{set}^{E_i}} \quad (\text{S98})$$

with γ_2 now

$$\gamma_2 = \frac{k_6 k_9 E_i^2}{\dot{k}_2} \quad (\text{S99})$$

Comparing A , A_{ss} and γ_n for the Different Controllers

Fig. S20 shows A , A_{ss} and γ_n for the zero-order ($n=0$), first-order ($n=1$), and second-order ($n=2$) controllers when k_2 increases linearly. In general there is a good agreement between the numerically calculated A from the rate equations and the calculated steady states A_{ss} . The second-order type of controller has high and increasing γ_2 values, which keeps A for this controller

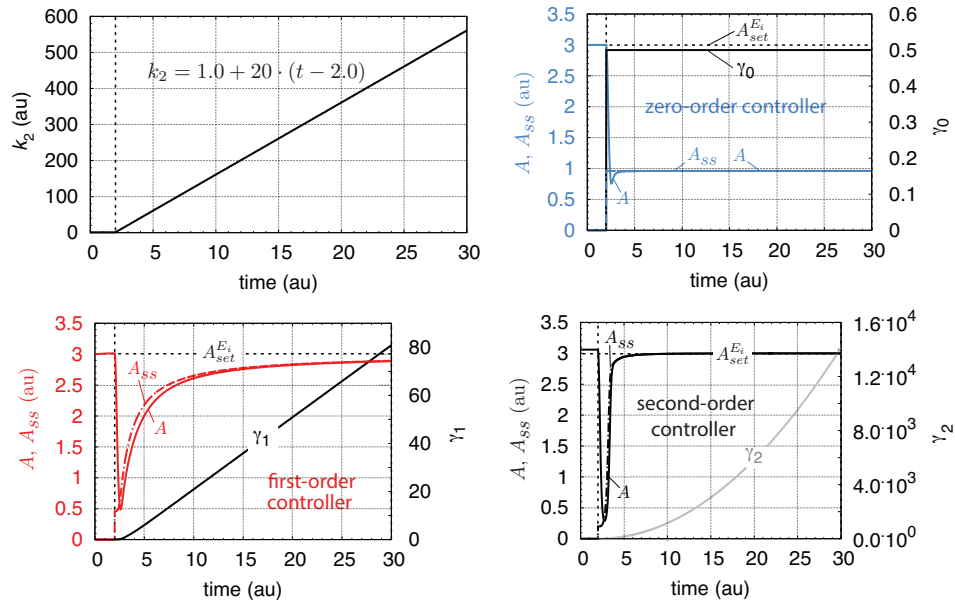


Figure S20: Comparison between stationary solution A_{ss} and numerical solution A and the offset contributions γ_n for the three integral control implementations in motif 3 when k_2 increases linearly.

close to $A_{set}^{E_i}$. This can be seen when inspecting the quadratic equation for A_{ss} :

$$A_{ss}^2 + A(\gamma_n + k_{24}) - \gamma_n \cdot A_{set}^{E_i} = 0 \quad (S100)$$

When γ_n becomes very large in comparison to A_{ss}^2 and k_{24} then Eq. S100 can approximately be written as

$$A_{ss} \cdot \gamma_n - \gamma_n \cdot A_{set}^{E_i} = 0 \quad \Rightarrow \quad A_{ss} = A_{set}^{E_i} \quad (S101)$$

showing that A_{ss} is close to $A_{set}^{E_i}$.

Fig. S21 shows A , A_{ss} and γ_n for the different controllers when k_2 increases exponentially.

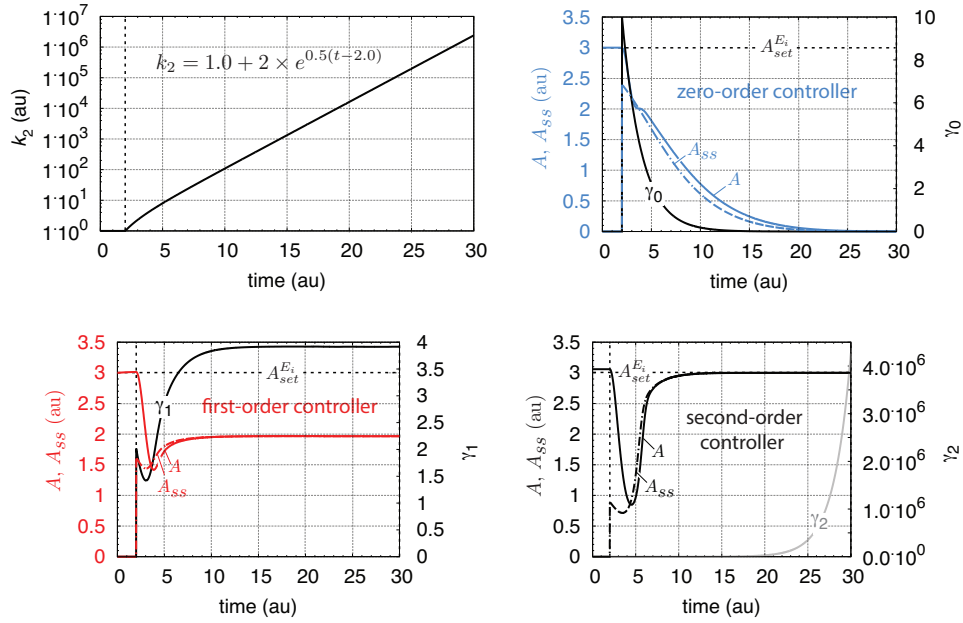


Figure S21: Comparison between stationary solution A_{ss} and numerical solution A and the offset contributions γ_n for the three integral control implementations in motif 3 when k_2 increases exponentially.

The zero-order controller is not able to defend the exponential growth of k_2 at all, while the first-order type of controller shows a constant offset contri-

bution γ_1 . Only the second-order controller is able to defend its set-point while γ_2 is constantly increasing such that A_{ss} is close to $A_{set}^{E_i}$ (Eq. S101).

Fig. S22 shows A , A_{ss} and the γ_n for the different controllers when k_2 increases hyperbolically.

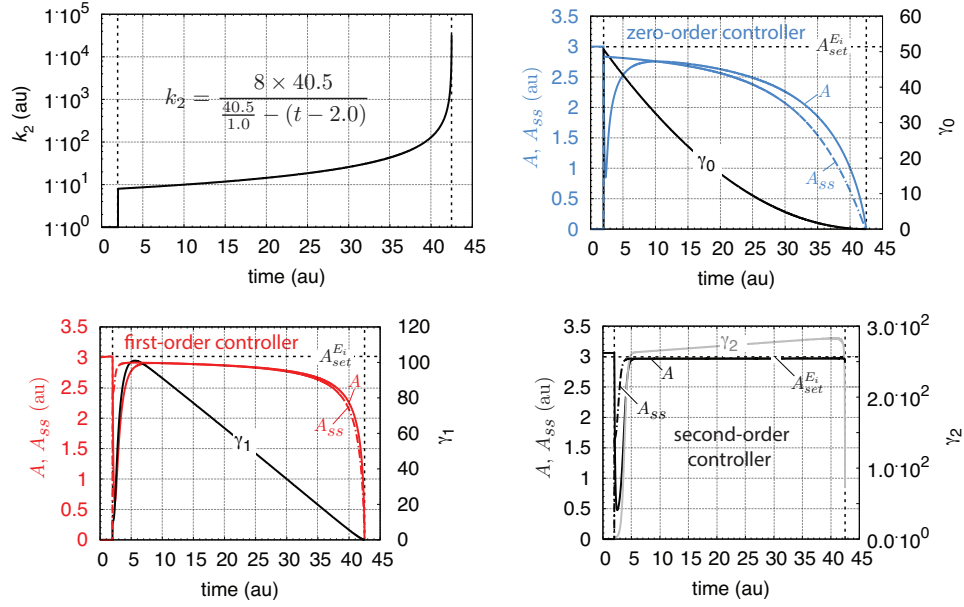


Figure S22: Comparison between stationary solution A_{ss} and numerical solution A and the offset contributions γ_n for the three integral control implementations in motif 3 when k_2 increases hyperbolically.

Only the second-order type of controller is able to defend its set-point during the hyperbolic increase of k_2 with a minor offset from $A_{set}^{E_i}$.

Supporting Information 7

Comparing Stationary and Numerical Solutions of A with the Different Implementations of Integral Control for Motif 7

Fig. S23 indicates the three implementations of integral control in motif 7.

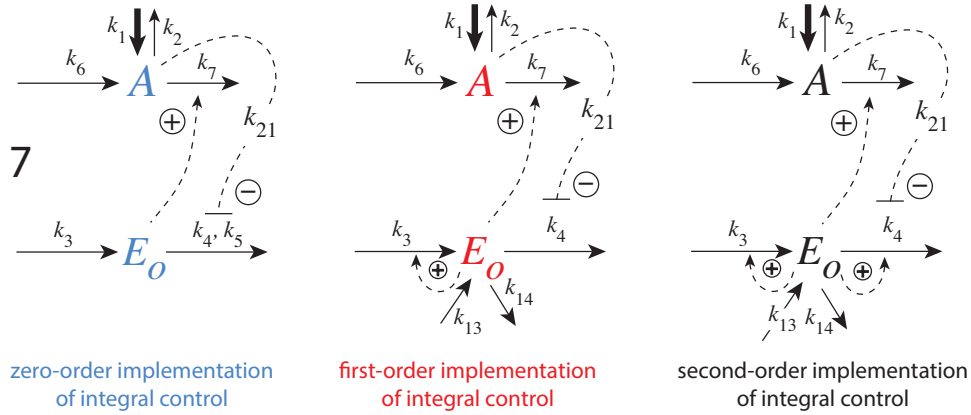


Figure S23: Reaction schemes of motif 7 with three implementations of integral control.

Zero-order Implementation of Integral Control

The rate equations for the zero-order type of controller (Fig. S23, left panel outlined in blue) are as follows, where k_{21} and k_5 play the role of an inhibition constant and a Michaelis constant, respectively:

$$\dot{A} = k_1 + k_6 - k_2 \cdot A - k_7 \cdot A \cdot E_o \quad (\text{S102})$$

$$\dot{E}_o = k_3 - \frac{k_4 \cdot E_o}{k_5 + E_o} \cdot \frac{k_{21}}{k_{21} + A} \quad (\text{S103})$$

The set-point of A is calculated for ideal zero-order condition with respect to E_o (Eq. S103), i.e., $k_5 \ll E_o$ such that

$$\dot{E}_o = k_3 - k_4 \cdot \frac{k_{21}}{k_{21} + A} \quad (\text{S104})$$

Setting Eq. S104 to zero gives the set-point $A_{set}^{E_o}$ as the steady state value A_{ss}

$$A_{set}^{E_o} = A_{ss} = k_{21} \left(\frac{k_4}{k_3} - 1 \right) \quad (\text{S105})$$

In the calculations below the set-point for the motif 7 controllers is $A_{set}^{E_o} = 6.0$.

To calculate A_{ss} when $\dot{k}_1 \neq 0$ and $\dot{E}_o \neq 0$ we take the double derivative of A with respect to time and assume that $\dot{A} = 0$ and $\ddot{A} = 0$

$$\ddot{A} = \dot{k}_1 - k_7 \dot{E}_o A \quad (\text{S106})$$

By inserting Eq. S103 into Eq. S106 with the assumption that $k_5 \ll E_o$ and setting the resulting equation to zero we get

$$\dot{k}_1 - k_7 \cdot A_{ss} \left(k_3 - \frac{k_4 \cdot k_{21}}{k_{21} + A_{ss}} \right) = 0 \quad (\text{S107})$$

which can be written in a quadratic form as

$$A_{ss}^2 - A_{ss} \left(\frac{k_4}{k_3} k_{21} - k_{21} + \frac{\dot{k}_1}{k_3 k_7} \right) - \frac{\dot{k}_1 k_{21}}{k_3 k_7} = 0 \quad (\text{S108})$$

Using $A_{set}^{E_o} = (k_4/k_3)k_{21} - k_{21}$, we rewrite Eq. S107 as

$$A_{ss}^2 - A_{ss} (A_{set}^{E_o} + \gamma_0) - \gamma_0 k_{21} = 0 \quad (\text{S109})$$

with

$$\gamma_0 = \frac{\dot{k}_1}{k_3 k_7} \quad (\text{S110})$$

The stationary solution A_{ss} is then given by:

$$A_{ss} = \left(\frac{A_{set}^{E_o} + \gamma_0}{2} \right) + \sqrt{\left(\frac{A_{set}^{E_o} + \gamma_0}{2} \right)^2 + 4k_{21}\gamma_0} \quad (\text{S111})$$

Equation S111 shows that when k_1 is constant ($\dot{k}_1 = 0$) then $\gamma_0 = 0$ and $A_{ss} = A_{set}^{E_o}$.

Autocatalytic Implementations of Integral Control

The stationary solutions for the two autocatalytic implementations of integral control are derived in an analogous manner as for Eq. S109. As an example we use the first-order autocatalytic implementation of integral control. The rate equations for A and E_o are:

$$\dot{A} = k_1 + k_6 - k_2 \cdot A - k_7 \cdot A \cdot E_o \quad (\text{S112})$$

$$\dot{E}_o = k_{13} - k_{14} \cdot E_o + k_3 \cdot E_o - k_4 \cdot E_o \cdot \frac{k_{21}}{k_{21} + A} \quad (\text{S113})$$

Neglecting in Eq. S113 the basal contributions of k_{13} and k_{14} to E_o , $A_{set}^{E_o}$ can be calculated by setting \dot{E}_o to zero, i.e.

$$\dot{E}_o = E_o \left(k_3 - k_4 \frac{k_{21}}{k_{21} + A_{ss}} \right) = 0 \quad (\text{S114})$$

Solving for A_{ss} and assuming that $E_o \neq 0$ gives the controller's set-point as in Eq. S105, i.e.,

$$A_{set}^{E_o} = A_{ss} = k_{21} \left(\frac{k_4}{k_3} - 1 \right) \quad (\text{S115})$$

In a similar manner $A_{set}^{E_o}$ for the second-order autocatalytic controller can be calculated leading to the same result as Eqs. S115 and S105.

To calculate A_{ss} for the first-order autocatalytic controller we take, as above, the double derivative of A with respect to time and assume that $k_1 \neq 0$ and $\dot{E}_o \neq 0$, together with $\dot{A} = \ddot{A} = 0$. The solution for A_{ss} for the first-order controller is analogous to Eq. S111

$$A_{ss} = \left(\frac{A_{set}^{E_o} + \gamma_1}{2} \right) + \sqrt{\left(\frac{A_{set}^{E_o} + \gamma_1}{2} \right)^2 + 4k_{21}\gamma_1} \quad (\text{S116})$$

where γ_1 is

$$\gamma_1 = \frac{\dot{k}_1}{k_3 k_7 E_o} \quad (\text{S117})$$

A_{ss} for the second-order controller can be calculated by Eq. S116 where γ_1 is replaced by γ_2

$$\gamma_2 = \frac{\dot{k}_1}{k_3 k_7 E_o^2} \quad (\text{S118})$$

Overview of the Performance of the Controllers

Fig. S24 gives an overview of the performance of controller motif 7 with the three implementations of integral control (Fig. S23).

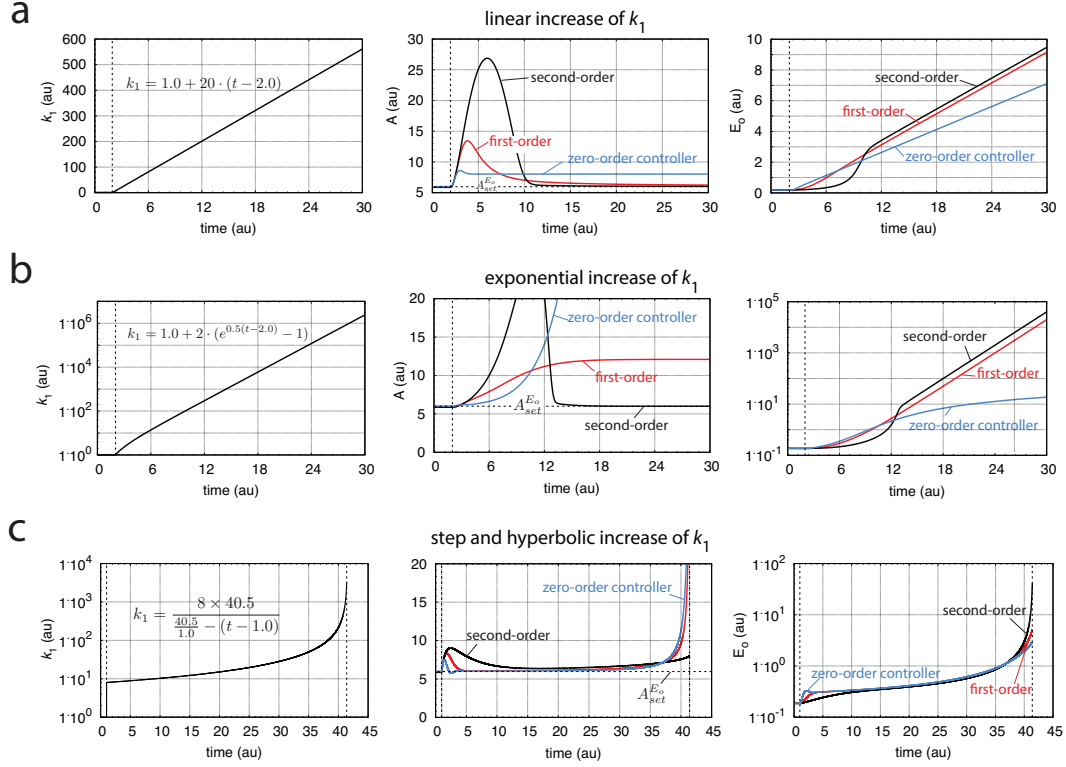


Figure S24: Performance of the three implementations of integral control for controller motif 7 (Fig. S23) when k_1 increases linearly (a, left panel), exponentially (b, left panel), and hyperbolically (c, left panel).

In case k_1 increases linearly, the zero-order controller (Fig. S24a, middle panel, outlined in blue) shows a constant deviation ("offset") in A from $A_{set}^{E_o}$. The offset arises, because the zero-order controller is able to compensate for

the linear increase in k_1 , but this takes some time. Since the zero-order controller cannot accelerate \dot{E}_o beyond a linear rate law, contrary to the first- and second-order controllers, the offset for the zero-order controller remains constant. Fig. S25 shows that the offset contribution γ_0 for the linear controller is constant while the corresponding γ_1 and γ_2 values for the first- and second-order controllers decrease in time and move A to $A_{set}^{E_o}$.

When k_1 increases exponentially (Fig. S24b, middle panel) the zero-order controller (outlined in blue) is not able to compensate for the k_1 increase. The first-order controller (outlined in red) is able to counteract the exponential k_1 increase, but because this controller's rate law can only be exponential the controller cannot accelerate \dot{E}_o beyond an exponential increase and therefore shows an offset in A . On the other hand, the second-order controller has an intrinsic hyperbolic rate law that can go beyond (be faster) than any exponential growth rate and has therefore the ability to reduce the offset, as seen by the decreasing γ_2 values for this controller (Fig. S26, second-order controller).

When k_1 increases hyperbolically the zero- and first-order controllers show better adaptation to $A_{set}^{E_o}$ than the second-order type of controller when \dot{k}_1 is still low. However, when \dot{k}_1 increases rapidly the second-order controller shows a much better performance, but with a considerable offset from $A_{set}^{E_o}$.

Rate constants and initial concentrations

The following rate constant values (in au) were used for all three type of controllers: k_1 , see Fig. S24; $k_2 = 0.0$, $k_3 = 1.0$, $k_4 = 61.0$, $k_5 = 1 \times 10^{-4}$, $k_6 = k_7 = 10.0$, $k_{13} = k_{14} = 1 \times 10^{-3}$, $k_{21} = 0.1$.

Initial concentrations for all three controllers: $A_0 = 6.0$, $E_{o,0} = 0.19$.

Comparing A , A_{ss} and γ_n for the Different Controllers

Fig. S25 shows A , A_{ss} and $\gamma_n = \dot{k}_1 / (k_3 k_7 E_o^n)$ ($n=0, 1$, or 2) for the different controllers when k_1 increases linearly. The γ_n values are an indicator for the difference between A and $A_{ss}^{E_o}$ ("offset") (Eq. S111). The constant γ_0 for the zero-order controller indicates a constant offset, while the decreasing γ_1 and γ_2 values for the first-order and second-order controllers indicate that these controllers have decreasing offsets and move A closer to $A_{ss}^{E_o}$.

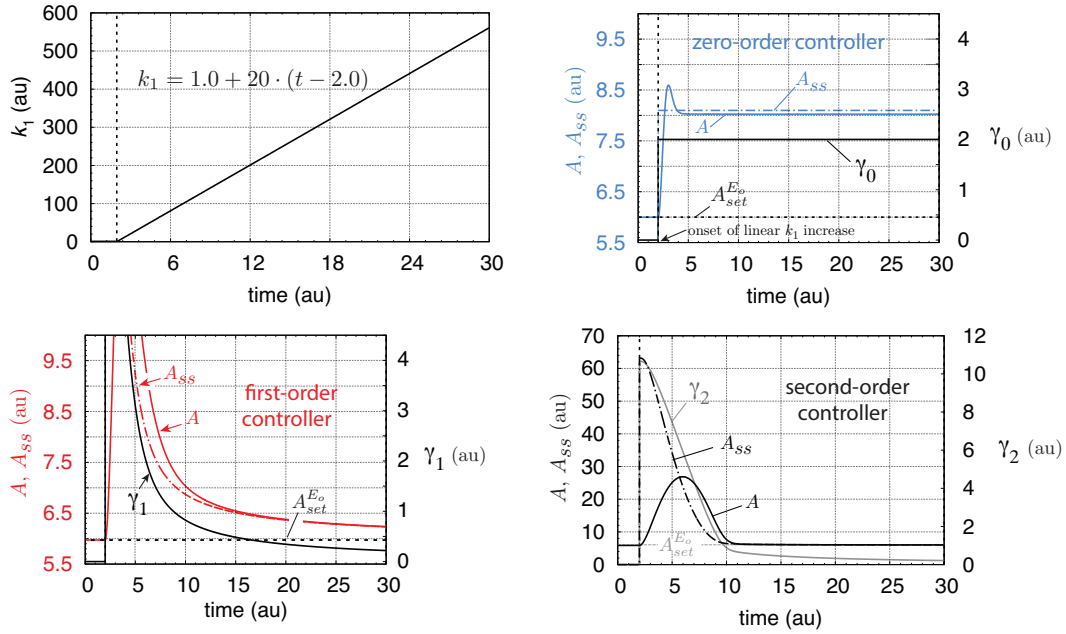


Figure S25: Comparison between stationary solution A_{ss} and numerical solution A and the offset contributions $\gamma_n = \dot{k}_1 / (k_3 k_7 E_o^n)$ for the three integral control implementations in motif 7 when k_1 increases linearly.

Fig. S26 shows A , A_{ss} and $\gamma_n = \dot{k}_1 / (k_3 k_7 E_o^n)$ ($n=0, 1$, or 2) for the different controllers when k_1 increases exponentially. The increasing γ_0 for the zero-order controller indicates the controller's breakdown.

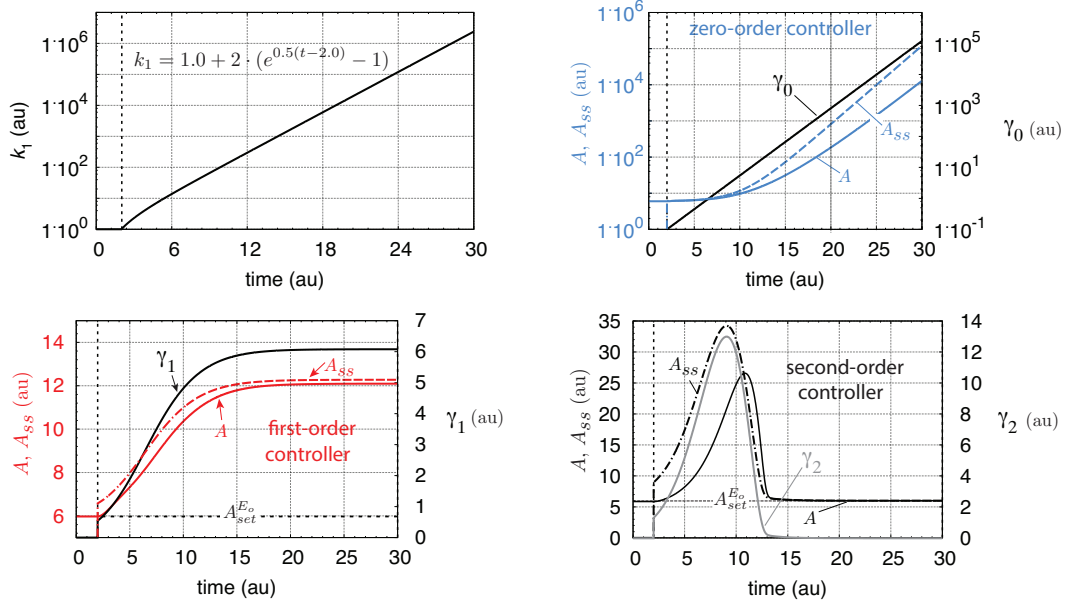


Figure S26: Comparison between stationary solution A_{ss} and numerical solution A and the offset contributions γ_n for the three integral control implementations in motif 7 when k_1 increases exponentially.

Fig. S27 shows A , A_{ss} and $\gamma_n = \dot{k}_1 / (k_3 k_7 E_o^n)$ ($n=0, 1$, or 2) for the different controllers when k_1 increases hyperbolically. Since all γ_n 's are increasing none of the controllers can successfully defend their set-points.

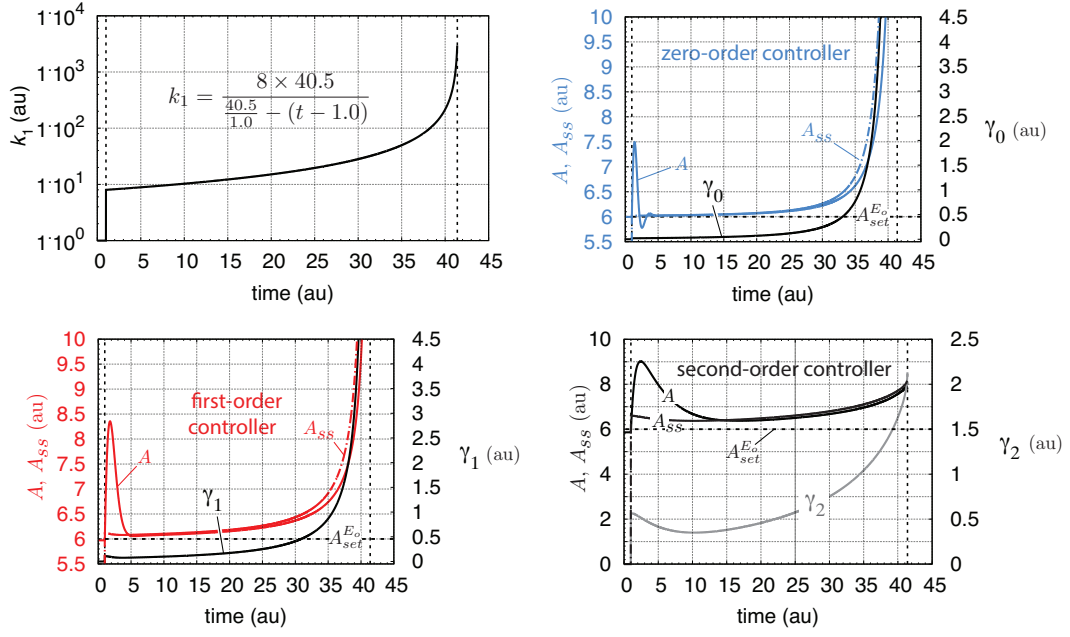


Figure S27: Comparison between stationary solution A_{ss} and numerical solution A and the offset contributions γ_n for the three integral control implementations in motif 7 when k_1 increases hyperbolically.

Supporting Information 8

Comparing Stationary and Numerical Solutions of A with the Different Implementations of Integral Control for Motif 8

Zero-Order Implementation of Integral Control

The reaction scheme of motif 8 is shown in Fig. 8 (main paper). The rate equations for the zero-order type of controller are:

$$\dot{A} = k_1 - k_2 \cdot A + k_6 - \frac{k_7 k_{22} A}{k_{22} + E_o} \quad (\text{S119})$$

$$\dot{E_o} = \frac{k_3 k_{21}}{k_{21} + A} - \frac{k_4 \cdot E_o}{k_5 + E_o} \quad (\text{S120})$$

The set-point of A is calculated as the steady state of A for constant k_1 and k_2 values when E_o is removed by zero-order kinetics, i.e., when $k_5 \ll E_o$ and $\dot{E_o}=0$:

$$\frac{k_3 k_{21}}{k_{21} + A_{ss}} - k_4 = 0 \quad (\text{S121})$$

Rearranging Eq. S121 gives

$$A_{set}^{E_o} = A_{ss} = k_{21} \left(\frac{k_3}{k_4} - 1 \right) \quad (\text{S122})$$

Stationary Solution of Zero-Order Controller for Increasing k_1

We assume that $\dot{A}=\ddot{A}=0$, while \dot{k}_1 and $\dot{E_o}$ are nonzero. Calculating \ddot{A} under these conditions we get

$$\ddot{A} = \dot{k}_1 + \frac{k_7 k_{22}}{(k_{22} + E_o)^2} \cdot \dot{E_o} \cdot A_{ss} = 0 \quad (\text{S123})$$

Inserting Eq. S120 into Eq. S123 and rearranging gives the following quadratic equation in A_{ss}

$$A_{ss}^2 + A_{ss} \cdot \underbrace{\left[k_{21} \left(1 - \frac{k_3}{k_4} \right) - \frac{\dot{k}_1(k_{22} + E_o)^2}{k_4 k_7 k_{22}} \right]}_{-A_{set}^{E_o}} = k_{21} \cdot \frac{\dot{k}_1(k_{22} + E_o)^2}{k_4 k_7 k_{22}} \quad (\text{S124})$$

Defining γ_n as

$$\gamma_n = \frac{\dot{k}_1(k_{22} + E_o)^2}{k_4 k_7 k_{22} E_o^n} \quad (\text{S125})$$

for $n = 0, 1, 2$ with respect to the zero-, first-, and second-order controllers, the solution of Eq. S124 (zero-order controller) is

$$A_{ss} = \frac{1}{2} A_{set}^{E_o} + \frac{\gamma_0}{2} + \sqrt{\left(\frac{A_{set}^{E_o}}{2} \right)^2 + \frac{1}{2} A_{set}^{E_o} \gamma_0 + \left(\frac{\gamma_0}{2} \right)^2 + k_{21} \gamma_0} \quad (\text{S126})$$

First-Order Implementation of Integral Control

The rate equations for the first-order type of controller are:

$$\dot{A} = k_1 - k_2 \cdot A + k_6 - \frac{k_7 k_{22} A}{k_{22} + E_o} \quad (\text{S127})$$

$$\dot{E}_o = \frac{k_3 k_{21} E_o}{k_{21} + A} - k_4 \cdot E_o \quad (\text{S128})$$

The (ideal) set-point of A is calculated as the steady state of A when $E_o \neq 0$ and $\dot{E}_o = 0$, i.e.:

$$\left(\frac{k_3 k_{21}}{k_{21} + A_{ss}} - k_4 \right) \cdot E_o = 0 \quad (\text{S129})$$

leading as in Eq. S122 to:

$$A_{set}^{E_o} = A_{ss} = k_{21} \left(\frac{k_3}{k_4} - 1 \right) \quad (\text{S130})$$

Stationary Solution of First-Order Controller for Increasing k_1

As above for the first-order type of controller, we assume that $\dot{A}=\ddot{A}=0$, while \dot{k}_1 and \dot{E}_o are nonzero. Calculating \ddot{A} under these conditions we get

$$\ddot{A} = \dot{k}_1 + \frac{k_7 k_{22}}{(k_{22} + E_o)^2} \cdot \dot{E}_o \cdot A_{ss} = 0 \quad (\text{S131})$$

Inserting Eq. S128 into Eq. S131 and rearranging gives the following quadratic equation in A_{ss}

$$A_{ss}^2 + A_{ss} \cdot \underbrace{\left[k_{21} \left(1 - \frac{k_3}{k_4} \right) - \gamma_1 \right]}_{-A_{set}^{E_o}} = k_{21} \cdot \gamma_1 \quad (\text{S132})$$

The solution for A_{ss} for the first-order type of controller when $\dot{k}_1 \neq 0$ and $\dot{E}_o \neq 0$ is given by:

$$A_{ss} = \frac{1}{2} A_{set}^{E_o} + \frac{\gamma_1}{2} + \sqrt{\left(\frac{A_{set}^{E_o}}{2} \right)^2 + \frac{1}{2} A_{set}^{E_o} \gamma_1 + \left(\frac{\gamma_1}{2} \right)^2 + k_{21} \gamma_1} \quad (\text{S133})$$

Second-Order Implementation of Integral Control

The rate equations for the second-order type of controller are:

$$\dot{A} = k_1 - k_2 \cdot A + k_6 - \frac{k_7 k_{22} A}{k_{22} + E_o} \quad (\text{S134})$$

$$\dot{E}_o = \frac{k_3 k_{21} E_o^2}{k_{21} + A} - k_4 \cdot E_o^2 \quad (\text{S135})$$

The ideal set-point of A is calculated as the steady state of A when $E_o \neq 0$ and $\dot{E}_o = 0$, i.e.:

$$\left(\frac{k_3 k_{21}}{k_{21} + A_{ss}} - k_4 \right) \cdot E_o^2 = 0 \quad (\text{S136})$$

leading as in Eqs. S122 and S130 to:

$$A_{set}^{E_o} = A_{ss} = k_{21} \left(\frac{k_3}{k_4} - 1 \right) \quad (\text{S137})$$

Stationary Solution of Second-Order Controller for Increasing k_1

The derivation for A_{ss} of the second-order controller is analogous to the derivations of the zero- and first-order controllers. A_{ss} for the second-order controller is

$$A_{ss} = \frac{1}{2}A_{set}^{E_o} + \frac{\gamma_2}{2} + \sqrt{\left(\frac{A_{set}^{E_o}}{2}\right)^2 + \frac{1}{2}A_{set}^{E_o}\gamma_2 + \left(\frac{\gamma_2}{2}\right)^2 + k_{21}\gamma_2} \quad (\text{S138})$$

Rate constants and initial concentrations

The following rate constant values (in au) were used for all three type of controllers: k_1 , see Fig. 9; $k_2 = 1.0$, $k_3 = 61.0$, $k_4 = 1.0$, $k_5 = 1 \times 10^{-7}$, $k_6 = 10.0$, $k_7 = 1 \times 10^3$, $k_{13} = k_{14} = 0.0$, $k_{21} = 0.1$, $k_{22} = 1 \times 10^{-2}$.

Initial concentrations for all three controllers: $A_0 = 6.00$, $E_{o,0} = 12.0$.

Comparing Stationary and Numerical Solutions of A

Linear Increase of k_1 with Time

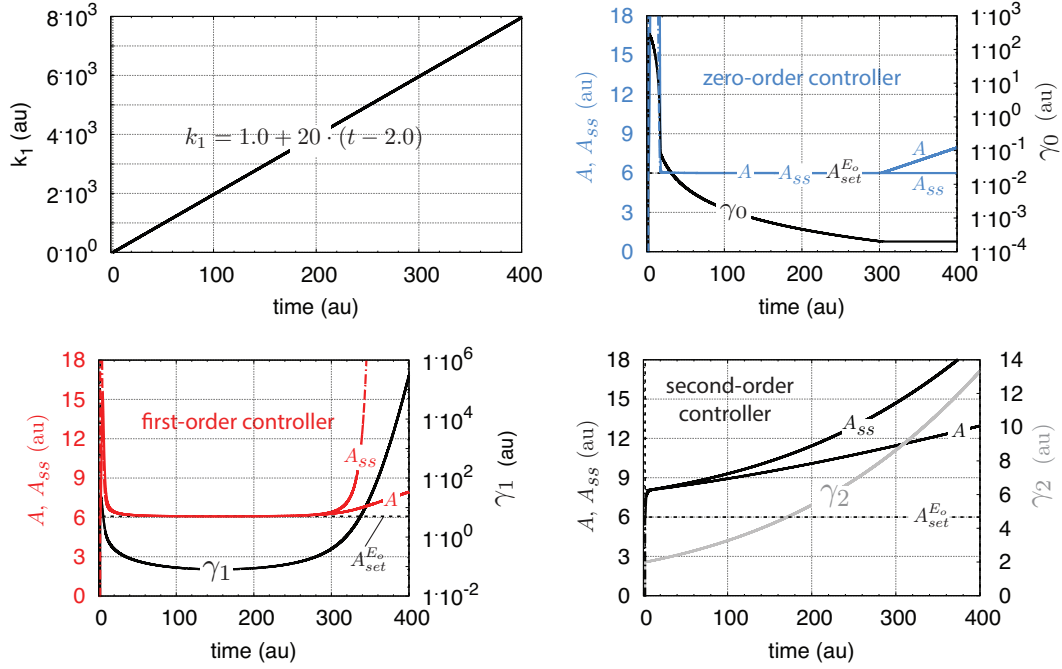


Figure S28: Comparison between stationary solutions A_{ss} and numerical solutions A and the offset contributions γ_n for the three integral control implementations in motif 8 when k_1 increases linearly with time.

Fig. S28 shows the A_{ss} and numerical A values for the zero-order type of controller 8 when k_1 increases linearly. The zero- and first-order type of controllers move their A concentrations close towards their homeostatic set-points as indicated by their decreasing γ_0 and γ_1 values. The second-order autocatalytic controller is not able to defend its homeostatic set-point indicated by the increasing γ_2 values.

Exponential Increase of k_1 with Time

During the exponential increase of k_1 none of the integral control implementations perform well as indicated by the increase of their γ_n values. Only the zero-order type of controller shows a temporary approach of A to $A_{set}^{E_o}$ as indicated by the decreasing γ_0 . However, as the concentration of E_o becomes too low to maintain the functionality of the negative feedback loop, the zero-order controller breaks down (Fig. 9b, right panel) and γ_0 increases.

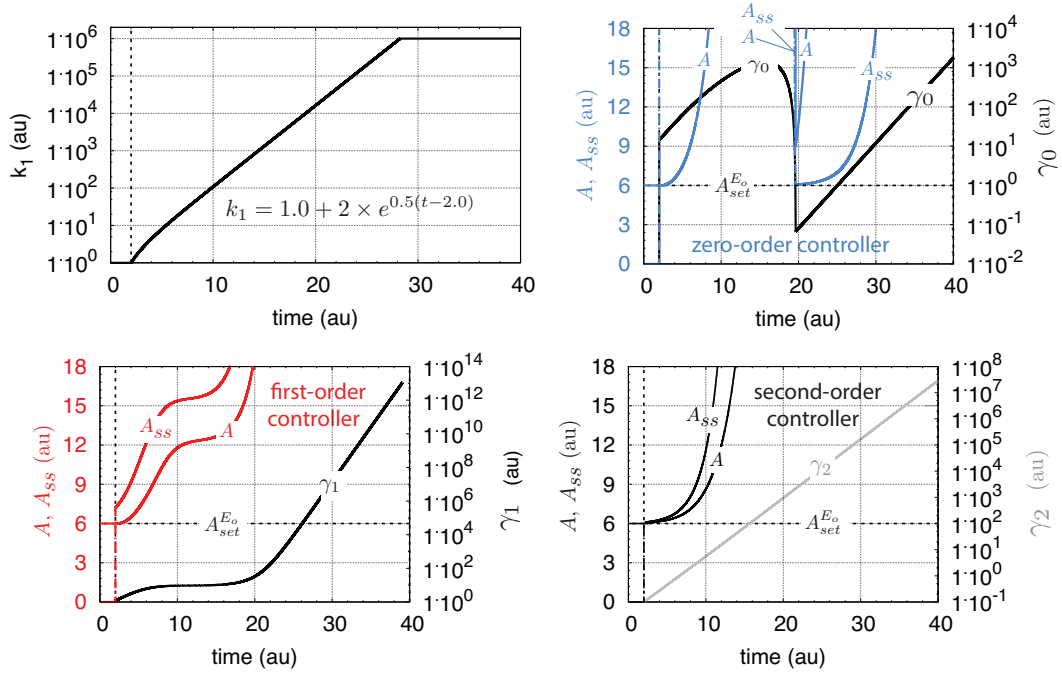


Figure S29: Comparison between stationary solutions A_{ss} and numerical solutions A and the offset contributions γ_n for the three integral control implementations in motif 8 when k_1 increases exponentially.

Hyperbolic Increase of k_1 with Time

Here k_1 undergoes at the start of the second phase a jump from 1 to 8 and then increases hyperbolically. Initially, the hyperbolic increase is relatively

slow and the controllers are able to adapt to the slowly increasing k_1 . The γ_n values of the three controllers is an indicator how the different controllers perform (Fig. S30). For the zero-order controller the initial γ_0 decrease indicates that the offset between A and $A_{set}^{E_o}$ decreases and A moves closer to $A_{set}^{E_o}$. However, as k_1 increases very rapidly near the border when k_1 approaches infinity, the controller breaks down and A increases rapidly with time.

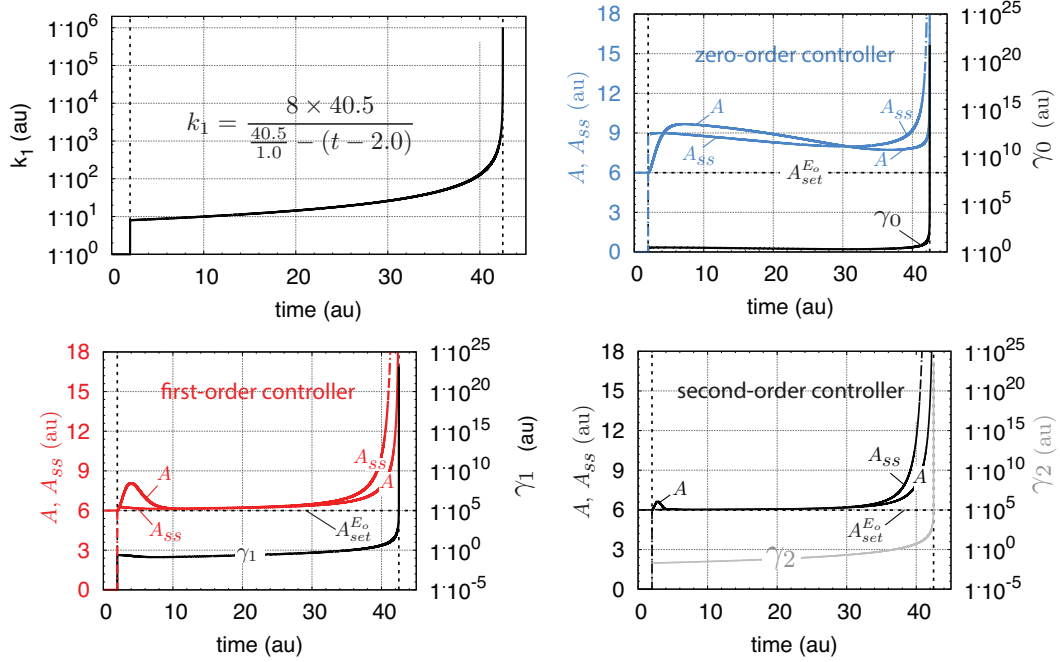


Figure S30: Comparison between stationary solution A_{ss} and numerical solution A and the offset contributions γ_n for the three integral control implementations in motif 8 when k_1 increases hyperbolically.

The first-order controller is able to cope with the initial decrease and has A values near $A_{set}^{E_o}$ for some time. However, the controller is not able maintain homeostasis as k_1 increases more and more rapidly and breaks down. While the second-order controller performs best and is able to hold its A value close to $A_{set}^{E_o}$ for the longest time, also this controller eventually breaks down when k_1 approaches rapidly infinity.

Supporting Information 9

Comparing Stationary and Numerical Solutions of A with the Different Implementations of Integral Control for Motif 4

Fig. S31 indicates the three implementations of integral control in motif 4.

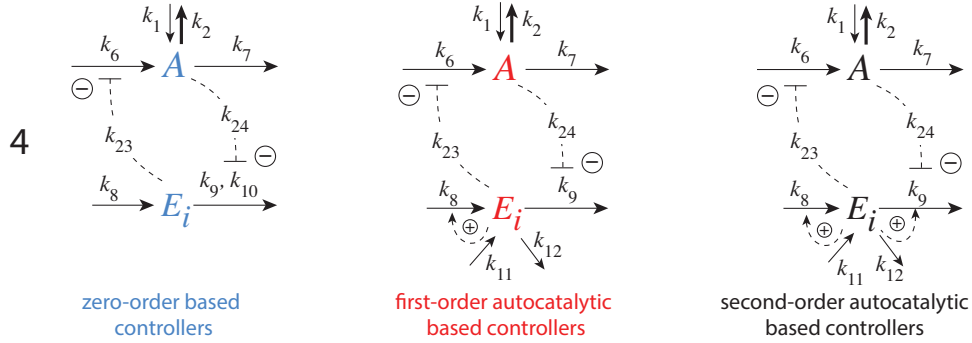


Figure S31: Reaction schemes of motif 4 with three implementations of integral control.

Zero-Order Implementation of Integral Control

The rate equations for the zero-order type of controller (Fig. S31, left panel outlined in blue) are as follows, where k_{23} and k_{24} play the roles of inhibition constants:

$$\dot{A} = k_1 - k_2 \cdot A + \frac{k_6 k_{23}}{(k_{23} + E_i)} - k_7 \cdot A \quad (\text{S139})$$

$$\dot{E}_i = k_8 - \frac{k_9 k_{24} E_i}{(k_{24} + A)(k_{10} + E_i)} \quad (\text{S140})$$

The set-point of A is calculated for ideal zero-order condition with respect to E_i (Eq. S140), i.e., $k_{10} \ll E_i$ such that $E_i/(k_{10} + E_i) = 1$ and Eq. S140 can

be rewritten as:

$$\dot{E}_i = k_8 - \frac{k_9 k_{24}}{(k_{24} + A)} \quad (\text{S141})$$

Setting Eq. S141 to zero gives the set-point $A_{set}^{E_i}$ as the steady state value A_{ss}

$$A_{set}^{E_i} = A_{ss} = k_{24} \left(\frac{k_9}{k_8} - 1 \right) \quad (\text{S142})$$

In the calculations which are given below we set $A_{set}^{E_i} = 3.0$.

To calculate A_{ss} when $\dot{k}_2 \neq 0$ and $\dot{E}_i \neq 0$, we take the double derivative of A with respect to time and assume that $\dot{A} = 0$ and $\ddot{A} = 0$

$$\ddot{A} = -\dot{k}_2 A_{ss} - \frac{k_6 k_{23}}{(k_{23} + E_i)^2} \dot{E}_i \quad (\text{S143})$$

By inserting Eq. S141 into Eq. S143 and setting it equal to zero, we get

$$\dot{k}_2 A_{ss} = \frac{k_6 k_{23} (k_9 k_{24} - k_8 k_{24} - k_8 A_{ss})}{(k_{23} + E_i)^2 (k_{24} + A_{ss})} = \frac{k_6 k_8 k_{23} (A_{set}^{E_i} - A_{ss})}{(k_{23} + E_i)^2 (k_{24} + A_{ss})} \quad (\text{S144})$$

where

$$k_9 k_{24} - k_8 k_{24} = k_8 k_{24} \left(\frac{k_9}{k_8} - 1 \right) = k_8 A_{set}^{E_i} \quad (\text{S145})$$

by using Eq. S142. Note that Eq. S144 implies that when $\dot{k}_2 = 0$ then $A_{ss} = A_{set}^{E_i}$.

Rearranging Eq. S144 leads to a quadratic expression in A_{ss}

$$A_{ss}^2 + \left(k_{24} + \frac{k_6 k_8 k_{23}}{\dot{k}_2 (k_{23} + E_i)^2} \right) A_{ss} - \frac{k_6 k_8 k_{23}}{\dot{k}_2 (k_{23} + E_i)^2} A_{set}^{E_i} = 0 \quad (\text{S146})$$

Introducing γ_n as

$$\gamma_n = \frac{k_6 k_8 k_{23} E_i^n}{\dot{k}_2 (k_{23} + E_i)^2} \quad (\text{S147})$$

where $n = 0, 1, 2$ for the zero-, first- and second-order controller, respectively, A_{ss} can be written as:

$$A_{ss} = - \left(\frac{k_{24} + \gamma_0}{2} \right) + \sqrt{\left(\frac{k_{24} + \gamma_0}{2} \right)^2 + \gamma_0 A_{set}^{E_i}} \quad (\text{S148})$$

In order to keep homeostasis in A the zero-order controller meets increasing k_2 values by decreasing E_i , which leads to increased γ_0 values. The offset $A_{set}^{E_i} - A_{ss}$ can be calculated by rearranging Eq. S146

$$A_{set}^{E_i} - A_{ss} = \frac{A_{ss}^2 + k_{24}A_{ss}}{\gamma_o} \quad (S149)$$

When $\gamma_0 \gg k_{24}A_{ss} + A_{ss}^2$ then $A_{ss} \approx A_{set}^{E_i}$.

Autocatalytic Implementations of Integral Control

The stationary solutions for the two autocatalytic implementations of integral control are derived in an analogous manner as for Eq. S146. For the first-order autocatalytic implementation of integral control the rate equations for A and E_i are:

$$\dot{A} = k_1 - k_2 \cdot A + \frac{k_6 k_{23}}{(k_{23} + E_i)} - k_7 \cdot A \quad (S150)$$

$$\dot{E}_i = k_{11} - k_{12} \cdot E_i + k_8 \cdot E_i - \frac{k_9 k_{24} E_i}{(k_{24} + A)} \quad (S151)$$

Neglecting in Eq. S151 the background synthesis and degradation contributions with respect to E_i by setting k_{13} and k_{14} to zero, $A_{set}^{E_i}$ can be calculated by setting \dot{E}_i to zero, i.e.

$$\dot{E}_i = E_i \left(k_8 - \frac{k_9 k_{24}}{(k_{24} + A_{ss})} \right) = 0 \quad (S152)$$

which leads to the same set-point as for the zero-order controller (Eq. S142), i.e.

$$A_{set}^{E_i} = A_{ss} = k_{24} \left(\frac{k_9}{k_8} - 1 \right) \quad (S153)$$

To calculate A_{ss} for the first-order controller when $\dot{k}_2 \neq 0$ and $\dot{E}_i \neq 0$, we take again the double derivative of A with respect to time and assume that $\dot{A}=0$ and $\ddot{A}=0$

$$\ddot{A} = -\dot{k}_2 A_{ss} - \frac{k_6 k_{23}}{(k_{23} + E_i)^2} \dot{E}_i = 0 \quad (S154)$$

By inserting Eq. S152 into Eq. S154 and setting it equal to zero we get

$$\dot{k}_2 A_{ss} = \frac{E_i k_6 k_{23} (k_9 k_{24} - k_8 k_{24} - k_8 A_{ss})}{(k_{23} + E_i)^2 (k_{24} + A_{ss})} = \frac{E_i k_6 k_8 k_{23} (A_{set}^{E_i} - A_{ss})}{(k_{23} + E_i)^2 (k_{24} + A_{ss})} \quad (S155)$$

where, as for Eq. S145, we use the expression for $A_{set}^{E_i}$

$$k_9 k_{24} - k_8 k_{24} = k_8 k_{24} \left(\frac{k_9}{k_8} - 1 \right) = k_8 A_{set}^{E_i} \quad (\text{S156})$$

Eq. S155 can be rearranged into the same quadratic equation as Eq. S146

$$A_{ss}^2 + (k_{24} + \gamma_1) A_{ss} - \gamma_1 A_{set}^{E_i} = 0 \quad (\text{S157})$$

with the solution

$$A_{ss} = - \left(\frac{k_{24} + \gamma_1}{2} \right) + \sqrt{\left(\frac{k_{24} + \gamma_1}{2} \right)^2 + \gamma_1 A_{set}^{E_i}} \quad (\text{S158})$$

using γ_1 from Eq. S147

For the second-order controller A_{ss} is calculated by Eq. S158 where γ_1 is replaced by γ_2 .

Overview of the Performance of the Controllers

Fig. S32 gives an overview of the performance of controller motif 4 with the three implementations of integral control (Fig. S31). In case k_2 increases linearly, the zero-order controller (Fig. S32a, middle panel, outlined in blue) performs best. The γ_0 value is considerably larger than γ_1 and γ_2 (see Fig. S33) leading to negligible offsets (Eq. S149). The zero-order controller also performs best when k_2 increases exponentially (Fig. S32b, middle panel) or even hyperbolically (Fig. S32c, middle panel) indicated by the higher γ_0 value of the zero-order controller in comparison with the other controllers.

Rate constants and initial concentrations

The following rate constant values (in au) were used for all three type of controllers: $k_1 = 1.0$, k_2 , see Figs. S32; $k_6 = 1 \times 10^4$, $k_7 = 10.0$, $k_8 = 1.0$, $k_9 = 31.0$, $k_{10} = 1 \times 10^{-4}$, $k_{11} = k_{12} = 0.0$, $k_{23} = 1 \times 10^{-4}$, $k_{24} = 0.1$.

Initial concentrations for all three controllers: $A_0 = 3.0$, $E_{i,0} = 0.03$.

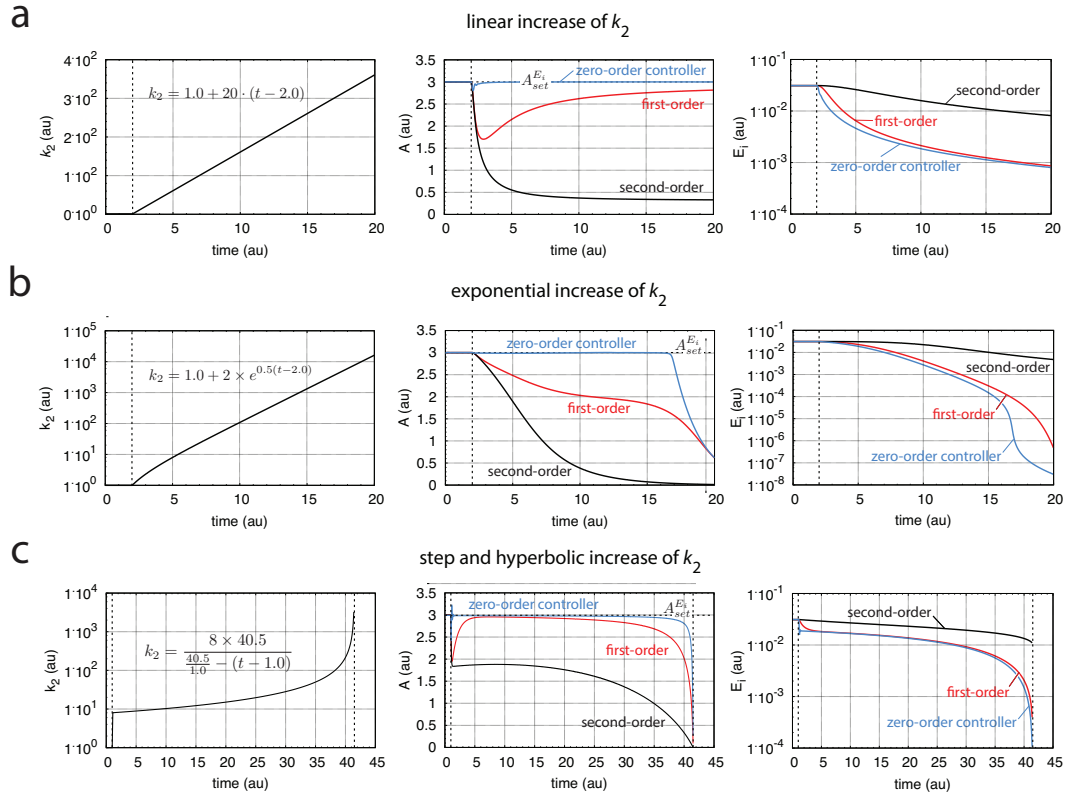


Figure S32: Performance of the three implementations of integral control (Fig. S31) for controller motif 4 when k_2 increases linearly (a, left panel), exponentially (b, left panel), and hyperbolically (c, left panel).

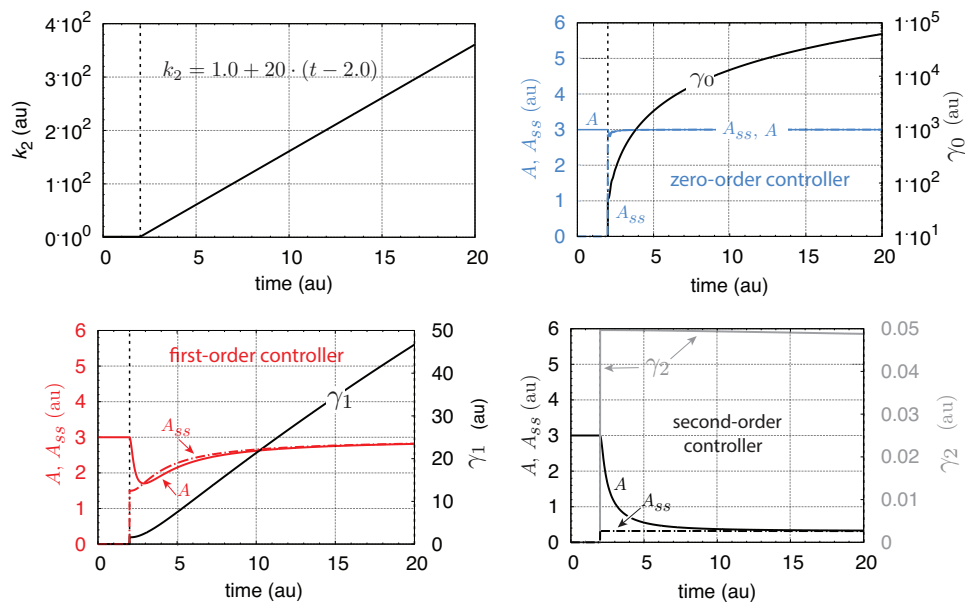


Figure S33: Comparison between stationary solutions A_{ss} , the numerical solutions A , and γ_n for the three integral control implementations in motif 4 when k_2 increases linearly.

Comparing A , A_{ss} and γ_n for the Different Controllers

Fig. S33 shows A , A_{ss} and the γ_n values for the different controllers when k_2 increases linearly. The zero-order and first-order controllers perform better than the second-order controller as indicated by the larger and increasing γ_0 and γ_1 values. In comparison with the first-order controller the zero-order controller shows higher γ_0 values and a more rapid adaptation to the set-point.

Fig. S34 shows A , A_{ss} and the γ_n values for the different controllers when k_2 increases exponentially. During the exponential increase of k_2 the zero-order controller defends its set-point, while both autocatalytic controllers perform poorly (Fig. S32b, middle panel), which is also indicated by the decreasing γ_1 and γ_2 values.

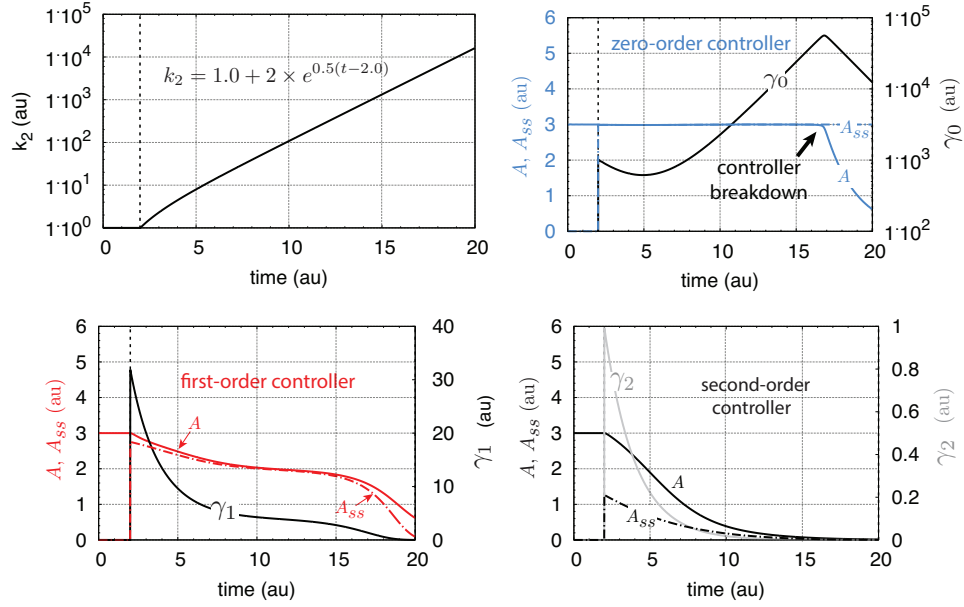


Figure S34: Comparison between stationary solutions A_{ss} , the numerical solutions A , and γ_n for the three integral control implementations in motif 4 when k_2 increases exponentially.

Fig. S35 shows A , A_{ss} and γ_n for the different controllers when k_2 increases hyperbolically. In this case all controllers show decreasing γ values. For the zero-order controller and also for the first-order controller γ_0 and γ_1 are relatively large, which keep the A values of these controllers close to $A_{set}^{E_i}$. When k_2 increases rapidly (above 40 time units) both the zero-order and first-order controllers break down, but the zero-order controller stays closer to $A_{set}^{E_i}$ than the other controllers (Fig. S32c, middle panel). The second-order autocatalytic controller performs less well with A values well below $A_{set}^{E_i}$.

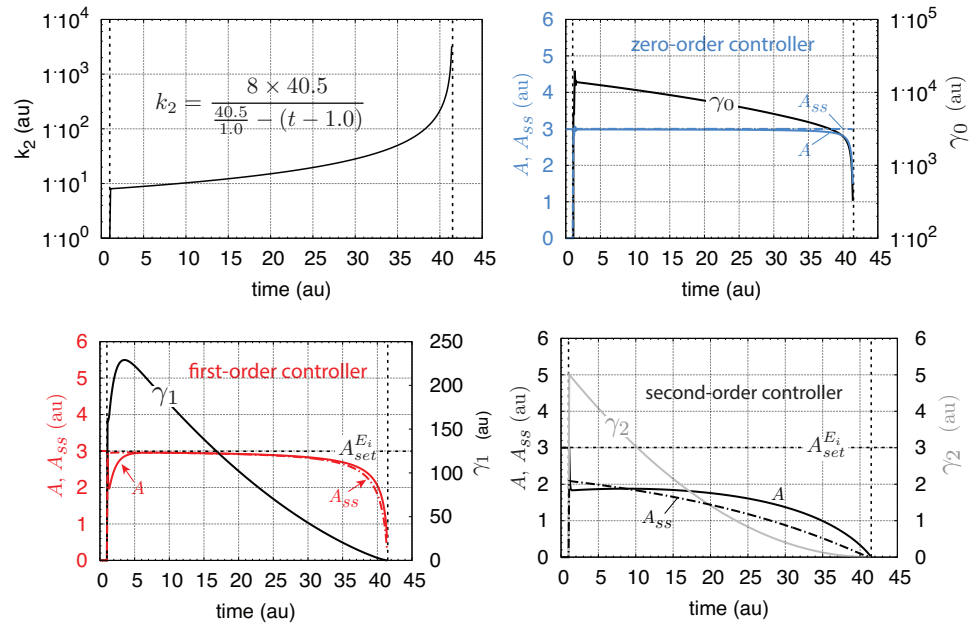


Figure S35: Comparison between stationary solutions A_{ss} , the numerical solutions A , and γ_n for the three integral control implementations in motif 4 when k_2 increases hyperbolically.